Title

P3N-PIPO, a Frameshift Product from *P3*, Pleiotropically Determines the Virulence of Clover Yellow Vein Virus in both Resistant and Susceptible Peas

Go Atsumi[a,b,c]#, Haruka Suzuki[a], Yuri Miyashita[a], Sun Hee Choi[a], Yusuke Hisa[a], Shunsuke Rihei[a], Ryoko Shimada[a], Eun Jin Jeon[a], Junya Abe[a], Kenji S. Nakahara[a,d]#, Ichiro Uyeda[a,d]

Graduate School of Agriculture, Hokkaido University, Sapporo, Hokkaido, Japan[a]; Iwate Biotechnology Research Center, Kitakami, Iwate, Japan[b]; National Institute of Advanced Industrial Science and Technology, Sapporo, Hokkaido, Japan[c]; Research Faculty of Agriculture, Hokkaido University, Sapporo, Japan[d]

Running Head: ClYVV P3N-PIPO is a pleiotropic virulence determinant

#Address correspondence to Go Atsumi, go-atsumi@aist.go.jp, or Kenji S. Nakahara, knakahar@res.agr.hokudai.ac.jp.

Word count for Abstract: 245

Word count for text (excluding references, table footnotes, and figure legends): 9138

ABSTRACT

Peas carrying the *cyv1* recessive resistance gene are resistant to clover yellow vein virus (ClYVV) isolates No. 30 and 90-1 (Cl-No.30 and Cl-90-1), but can be infected by a derivative of Cl-90-1 (Cl-90-1 Br2). The main determinant for the breaking of *cyv1* resistance by Cl-90-1 Br2 is P3N-PIPO produced from the *P3* gene via transcriptional slippage, and the higher level of P3N-PIPO produced by Cl-90-1 Br2 than by Cl-No.30 contributes to the breaking. Here we show that P3N-PIPO is also a major virulence determinant in susceptible peas that possess another resistance gene, *Cyn1*, which does not inhibit systemic infection with ClYVV but causes hypersensitive reaction–like lethal systemic cell death. We previously assumed that the susceptible pea cultivar PI 226564 has a weak allele of *Cyn1*. Cl-No.30 did not induce cell death but Cl-90-1 Br2 killed the plants. Our results suggest that P3N-PIPO is recognized by *Cyn1* and induces cell death. Unexpectedly, heterologously strongly expressed P3N-PIPO of Cl-No.30 appears to be recognized by *Cyn1* in PI 226564. P3N-PIPO accumulation from the *P3* gene of Cl-No.30 was significantly lower than that from Cl-90-1 Br2 in a *Nicotiana benthamiana* transient assay. Therefore, *Cyn1*-mediated cell death also appears to be determined by the level of P3N-PIPO. The more efficiently a ClYVV isolate broke *cyv1* resistance, the more it induced cell death systemically (resulting in a loss of environment for virus accumulation) in susceptible peas carrying *Cyn1*, suggesting that antagonistic pleiotropy of P3N-PIPO controls the resistance breaking of ClYVV.

IMPORTANCE

Control of plant viral disease has relied on the use of resistant cultivars; however, emerging mutant viruses have broken many types of resistance. Recently, we revealed that Cl-90-1 Br2 breaks the recessive resistance conferred by *cyv1*, mainly by accumulating a higher level of P3N-PIPO than the non-breaking isolate Cl-No.30. Here, we show that a susceptible pea line

recognized the increased P3N-PIPO amount produced by Cl-90-1 Br2 and activated the salicylic-acid-mediated defense pathway, inducing lethal systemic cell death. We found a gradation of virulence among ClYVV isolates in *cyv1* pea and two susceptible peas. This study suggests a trade-off between breaking of recessive resistance (*cyv1*) and host viability; the latter is presumably regulated by the dominant *Cyn1* gene, which may impose evolutionary constraints upon *P3N-PIPO* for overcoming resistance. We propose a working model of the host strategy to sustain the durability of resistance and control fast-evolving viruses.

INTRODUCTION

Host plants protect themselves from virus infection by activating defense systems mediated by immune receptors (e.g., nucleotide-binding site (NB)–leucine-rich repeat (LRR) proteins) (1). Plants have many NB-LRR immune receptors, each of which recognizes specific viral proteins. The activated immune response is referred to as a hypersensitive response (HR) and is often accompanied by cell death. When HR is induced, the virus is localized in and around the infection locus. NB-LRR immune receptors are encoded in resistance genes that are genetically dominant.

Another important defense against plant virus infection is genetically recessive resistance (2). The viral life cycle totally relies on the host cells, and viruses require host factors in order to multiply within cells and move to neighboring cells. Therefore, the lack of a specific host co-opted factor required for the viral life cycle leads to host resistance against the virus. Many natural recessive resistances against viruses have been identified in diverse crops (2). Extensive studies have been carried out against the viruses belonging to *Potyvirus*, the major genus in the *Potyviridae* family, which is one of the two largest plant virus genera and found in most climatic regions worldwide (3). These viruses infect a broad range of host plants including both monocots and dicots. They cause considerable crop damage, resulting in severe economic losses. Most of the recessive resistance genes against members of genus *Potyvirus* have been identified as encoding eukaryotic initiation factors such as eIF4E. Host eIF4E binds viral VPg protein that is covalently attached to the 5′ end of viral genomic RNA, and the complex initiates the translation of viral protein (4). For example, *cyv2* in pea confers recessive resistance to clover yellow vein virus (ClYVV), which causes severe damage to important legume crops including French bean, broad bean, and pea. A previous study showed that the resistance to ClYVV conferred by *cyv2* is mediated by eIF4E (5).

There is another recessive gene, *cyv1*, that confers resistance to ClYVV in pea (6). ClYVV No.30 isolate (Cl-No.30) cannot infect PI 429853 carrying *cyv1*, but ClYVV 90-1 Br isolate (Cl-90-1 Br2) can infect systemically (7) (Table 1). Our previous analysis revealed that P3N-PIPO, which consists of the N-terminal amino acids of P3 followed by a small peptide called PIPO encoded in the +2 reading frame (8-10), is a major determinant for breaking of *cyv1* resistance (7). We suggested that higher accumulation of P3N-PIPO in Cl-90-1 Br2 than in Cl-No.30 contributes to the breaking of resistance (7). P3N-PIPO has an essential role in virus cell-to-cell movement (10). Three independent groups including our own recently showed that P3N-PIPO is produced mainly by transcriptional slippage within the *P3* gene (11-13).

Plant viruses continually evolve and gain virulence, which enables them to inhibit or escape plant defense/resistance systems. Although higher virulence is favorable for virus adaptation, extremely high virulence (i.e., induction of lethal systemic cell death) seems to be a disadvantage for virus survival because the virus loses an environment in which to propagate if the host cells are dead. Several examples of excessively high virulence have been reported. Soybean mosaic virus (SMV) strain G7 induces cell death systemically and kills the host plant (14). The turnip mosaic virus (TuMV) TuR1 isolate induces lethal systemic cell death in *A. thaliana* accession Landsberg *erecta* (L*er*) (15). It was shown that the systemic cell death caused by SMV or TuMV is a form of HR that is regulated by *Rsv1* or *TuNI* in soybean or *A. thaliana* L*er*, respectively (16, 17). It was suggested that both *Rsv1* and *TuNI* encode NB-LRR resistance proteins (18, 19). These reports and others lead us to propose that extremely high virulence, an unfavorable state for the virus, is controlled genetically by host plants.

Extremely high virulence of ClYVV has been observed in many pea cultivars: ClYVV systemically induces cell death, resulting in plant death within 2 weeks when used to

infect young plants (20-22) (Table 1). We previously reported that the cell death induced by Cl-No.30 in pea PI 118501 is a form of HR-like response accompanied by the activation of the salicylic acid (SA) pathway, which is one of the hallmarks of HR (20). However, Cl-No.30 infection is not localized and induces cell death systemically. A genetic study in pea suggested that this cell death is controlled by a single dominant locus called *Cyn1* (21). *Cyn1* is suggested to be an NB-LRR gene whose product recognizes Cl-No.30 and induces HR associated with cell death (20, 21).

We previously revealed that Cl-90-1 Br2, a mutant isolate that originated from Cl-90-1, breaks *cyv1* recessive resistance in pea (7) (Table 1). In the present study, we revealed that Cl-90-1 Br2 induced lethal systemic cell death and found that P3N-PIPO, but not P3, was a major determinant of the induction of cell death in PI 226564. This was discovered by infection of PI 226564 with chimeric ClYVVs and by transient assays using white clover mosaic virus (WClMV) vectors. We showed that P3N-PIPO is quantitatively and/or qualitatively involved in cell death induction in pea by using chimeric and mutant ClYVVs and by transient assays in *N. benthamiana*. Chimeric P3N-PIPO expression analysis by using WClMV indicated that the PIPO peptide was not the sole determinant of cell death induction. Finally, we showed a consistent gradation of virulence among ClYVV isolates in *cyv1* peas (recessive resistance) and two susceptible peas. This study, combined with our previous studies (7), shows that P3N-PIPO is involved in both breaking of recessive resistance and disease expression. We suggest that the pleiotropic effects of P3N-PIPO in determining ClYVV virulence in pea result in a trade-off between breaking of recessive resistance (*cyv1*) and maintenance of host viability, which is presumably controlled by a *Cyn1*-mediated immune response.

MATERIALS AND METHODS

Preparation of plasmid constructs and infectious clones

Sequences of the primers used for vector construction are available upon request. The construction of ClYVV chimeric clones Cl-P1HC, Cl-BB, Cl-NS, Cl-SB, Cl-RB, and Cl-RB^{M28R} with *GFP* (=RB/P3&P3N-PIPO^{M28R} in (7)) was described previously (7). To make Cl-RB without *GFP*, the *Sal*I–*Bam*HI fragment of Cl-BB with *GFP* was used to replace that of Cl-RB with *GFP*. To make Cl-RB+P1HC without *GFP*, the *Sal*I–*Bam*HI fragment of Cl-BB with *GFP* was used to replace that of Cl-RB+P1HC with *GFP*; Cl-RB+P1HC with *GFP* was made by replacing the *Bgl*II (*HC-Pro*)–*Bgl*II (*P3*) fragment of Cl-BB carrying *GFP* with that of Cl-P1HC with *GFP*. To make Cl-RB+NS without *GFP*, the *Eco*RV–*Bgl*II (HC-Pro) fragment of pClYVV-Pst/CP (23) was used to replace that of Cl-RB+NS with *GFP*; Cl-RB+NS with *GFP* was made by replacing the *Bgl*II (*HC-Pro*)–*Nhe*I (*P3*) fragment of Cl-RB containing *HC-Pro* of Cl-No.30 and *P3* of Cl-90-1 Br2 with that of Cl-NS with *GFP*. To replace the *Bgl*II–*Nhe*I fragment, two *Nhe*I sites within the *Bgl*II–*Nhe*I fragment of Cl-90-1 Br2 were disrupted by site-directed mutagenesis to generate BgNhΔNh. BgNhΔNh was amplified with primers no.167 and no.196 using two overlapping fragments amplified with no.167/no.201 and no.202/no.196 as templates. To make Cl-RB+SB without *GFP*, the *Sal*I–*Bam*HI fragment of Cl-SB with *GFP* was used to replace that of Cl-RB without GFP. To make Cl-90-1 Br2-P3B$^{No.30}$ without *GFP*, the *Sal*I–*Bam*HI fragment of Cl-SB with *GFP* was used to replace that of Cl-P1HC with *GFP*, thus producing Cl-P1HC+SB without *GFP*, and then the *Nhe*I–*Sal*I fragment of Cl-NS with GFP was used to replace that of Cl-P1HC+SB without *GFP* to produce the final vector. Cl-90-1 Br2-P3B$^{No.30}$ without *GFP* contains an *Nhe*I site located upstream from the *Bgl*II site at the 3′ end of the P3B region, but the sequence of the region from the *Nhe*I site to the *Bgl*II site of Cl-90-1 Br2-P3B$^{No.30}$ without *GFP* is identical to that of Cl-No.30 except for a synonymous mutation (G [Cl-No.30] to A [Cl-90-1 Br2-P3B$^{No.30}$]) at nucleotide position 801 of the *P3* gene (7).

155 The WClMV vectors pWCl/P3N-PIPO-RB, pWCl/P3-RB, pWCl/P3ΔPIPO-RB,
156 and pWCl/GFP were constructed previously (24, 25). In this study, we constructed pWCl/P3-
157 No.30, pWCl/P3N-PIPO-No.30, pWCl/P3ΔPIPO-No.30, pWCl/P3N-PIPO-CS,
158 pWCl/P3N^{RB}-PIPO^{CS}, and pWCl/P3N^{CS}-PIPO^{RB}. For construction of pWCl/P3-No.30,
159 pWCl/P3N-PIPO-No.30, and pWCl/P3ΔPIPO-No.30, pClYVV/C3-S65T (26) was used as a
160 template. The *P3* fragment was obtained by PCR with primers no.3406/no.3412. The *P3N-*
161 *PIPO* fragment was amplified using primers no.3406/no.3415 from the mixture of two PCR
162 products amplified with primers no.3406/no.3653 and no.3652/no.3415. The length of *P3N-*
163 *PIPO* encoded in Cl-No.30 (647 nucleotides) is shorter than that encoded in Cl-RB (692
164 nucleotides) (7). We cloned *P3N-PIPO* of Cl-No.30 as a fragment from the 5' end of P3 to
165 the position corresponding to the stop codon of Cl-RB *PIPO* (located downstream from stop
166 codon of *PIPO* frame of Cl-No.30). *P3N-PIPO* has two mutations: (1) a G insertion in the A_6
167 sequence within the G_2A_6 motif which is expected to prevent transcriptional slippage or
168 ribosomal frameshift and translate P3N-PIPO as a zero-frame product, and (2) a G-to-A
169 substitution that introduces a stop codon in the *P3* frame but a silent mutation in the *PIPO*
170 frame (24). The *P3ΔPIPO* fragment was amplified using primers no.3406/no.3412 from the
171 mixture of two PCR products amplified with primers no.3406/no.3410 and no.3411/no.3412.
172 *P3ΔPIPO* has a stop codon in the *PIPO* frame but a silent mutation in the *P3* frame (24). For
173 construction of pWCl/P3N-PIPO-CS, a cDNA clone constructed from the BYMV CS isolate
174 (pBY-CS) (27) was used as a template. The *P3N-PIPO-CS* fragment was amplified using
175 primers no.3621/no.3622 from the mixture of two PCR products amplified with primers
176 no.3621/no.3669 and no.3668/no.3622. We cloned *P3N-PIPO* of BY-CS as a fragment from
177 5' to 3' end of *P3* gene carrying the same mutations introduced in *P3N-PIPO-RB* for enabling
178 P3N-PIPO to be translated as a zero-frame product. For construction of pWCl/P3N^{RB}-PIPO^{CS}
179 and pWCl/P3N^{CS}-PIPO^{RB}, pCl-RB (7) and pBY-CS (27) were used as templates. The *P3N^{RB}-*

PIPO^{CS} fragment was amplified using no.3945/no.3625 from the mixture of *P3N* of Cl-RB and *PIPO* of BY-CS amplified with no.3945/no.3885 and no.3955/no.3625, respectively. The *P3N*^{CS}-*PIPO*^{RB} fragment was amplified using no.3946/no.3409 from the mixture of *P3N* of BY-CS and *PIPO* of Cl-RB amplified with no.3946/no.3887 and no.3954/no.3409, respectively. For construction of *P3N*^{RB}-*PIPO*^{CS} and *P3N*^{CS}-*PIPO*^{RB}, we cloned from 5' end of *P3* to stop codon of *PIPO* frame. For *P3-No.30*, *P3N-PIPO-No.30*, *P3ΔPIPO-No.30*, and *P3N-PIPO-CS*, the cDNA fragments were introduced into the pGEM-T Easy plasmid (Promega, Fitchburg, WI), digested with *Spe*I and *Xho*I, and inserted into the WClMV vector (25) cut with the same restriction enzymes. For *P3N*^{CS}-*PIPO*^{RB}, the cDNA fragment introduced into the pGEM-T Easy plasmid was digested with *Nhe*I and *Xho*I and inserted into the WClMV vector cut with the same restriction enzymes. For *P3N*^{RB}-*PIPO*^{CS}, the cDNA fragment introduced into the pGEM-T Easy plasmid was cut with *Sac*II, and 5′ and 3′ ends of the plasmid were blunted using T4 DNA polymerase (TaKaRa Bio, Kusatsu, Japan). The blunted fragments were digested with *Xho*I and inserted into the WClMV vector cut with *Sma*I and *Xho*I.

The pTA/RB-P3(PIPO:FLAG^{-1}), pTA/No.30-P3(PIPO:FLAG^{-1}), pTA/RB-P3N-PIPO:FLAG^{mk}, and pTA/No.30-P3N-PIPO:FLAG^{mk} constructs were previously described (13).

All viral fragments were amplified using KOD-plus2 neo DNA polymerase (TOYOBO, Osaka, Japan) according to the manufacturer's instructions, and their nucleotide sequences were confirmed.

Plant growth conditions and viral infection

Pea (*Pisum sativum*), broad bean (*Vicia faba*), and *N. benthamiana* were cultivated in a growth chamber or growth room at 21–23°C with a 16-h photoperiod. Viral inocula were

prepared as described previously (20). For ClYVV, broad bean was inoculated with each infectious cDNA using particle bombardment. For WClMV, 1 μg of each WClMV plasmid was mechanically inoculated onto a susceptible pea line, PI 250438. The upper symptomatic leaves were harvested and ground in an inoculation buffer (0.1 M phosphate buffer, pH 7.0, and 1% 2-mercaptoethanol). The crude sap was mechanically inoculated onto the second and/or third leaves of 2-week-old pea plants. At the same time, all plants were inoculated with inoculation buffer alone as a negative control (mock inoculation).

Sequence alignment

P3N-PIPO amino acid (ClYVV, BYMV, and pea seed-borne mosaic virus [PSbMV]) sequences were aligned using MUSCLE (3.8) (http://www.ebi.ac.uk/Tools/msa/muscle/) (28). The amino acid sequences of P3N-PIPO were obtained by translating the sequences from the 5′ end of *P3* to the stop codon of *P3N-PIPO* after introducing an A into the A_{6-7} region in the $G_{1-2}A_{6-7}$ motif of each virus to shift the reading frame.

RNA extraction, reverse transcription, and real-time PCR

Pea leaves were homogenized in liquid nitrogen, and total RNA was isolated using TRIzol reagent (Thermo Fisher Scientific, Waltham, MA) according to the manufacturer's instructions. Each RNA sample was treated with RNase-free DNase I (Roche Diagnostics, Basel, Switzerland), and 1 μg of total RNA was reverse-transcribed using ReverTraAce (TOYOBO). The reaction mixture (20 μl) contained 100 units of ReverTraAce, 1 mM dNTP, 25 pmol random 9-mers, and 1–2 μg total RNA in 1× buffer. Samples were first incubated at 30°C for 10 min, then at 42°C for 30 min, and finally at 99°C for 5 min. Real-time PCR was performed using the DNA Engine Opticon 2 System (Bio-Rad Laboratories, Hercules, CA) as previously described (20). The reaction mixture (25 μl) contained 0.625 U of ExTaq

(TaKaRa), ExTaq buffer, 0.2 mM dNTP, 0.2 μM each of forward and reverse primers, SYBR Green (×30,000 dilution) (Thermo Fisher Scientific), and cDNA obtained by reverse transcribing 12.5 ng of total RNA. Samples were incubated for 5 min at 95°C; followed by 40 cycles of 95°C for 10 s, 53°C for *SA-CHI* (accession number L37876) or 55°C for *HSR203J* (AB026296) for 30 s, and 72°C for 20 s. Transcript levels were normalized to that of *18S rRNA* (U43011), and means and standard deviations were calculated. The primers used for real-time PCR were as follows: SA-CHI-F and SA-CHI-R for *SA-CHI*, HSR203J-F and HSR203J-R for *HSR203J*, and 18S rRNA-F and 18S rRNA-R for *18S rRNA*.

N. benthamiana leaves were homogenized in liquid nitrogen, and total RNA was isolated by the AGPC (acid guanidinium thiocyanate–phenol/chloroform) extraction method (29), followed by purification with a FARB column (Favorgen Biotech Corp, Ping-Tung, Taiwan). Total RNA was digested with TURBO DNase (Thermo Fisher Scientific) and reverse-transcribed using PrimeScript RTase (TaKaRa) according to the manufacturer's instructions. Real-time PCR was performed using the StepOnePlus system (Thermo Fisher Scientific). The reaction mixture (10 μl) contained KAPA SYBR FAST qPCR Kit Master Mix ABI Prism (Kapa Biosystems, Wilmington, MA), 0.3 μM each of forward and reverse primer, and cDNA obtained by reverse transcribing 50 ng of total RNA. Samples were incubated for 20 s at 95°C, followed by 40 cycles of 95°C for 3 s and 60°C for 30 s. Transcript levels of *P3N-PIPO-FLAG* were normalized to that of *NbEF1α* (AY206004). The primers used were as follows: GGS4-3FL-F and GGS4-3FL-R for *P3N-PIPO-FLAG*, NbEF1α-F and NbEF1α-R for *NbEF1α*. Primers were designed in a region of *P3N-PIPO-FLAG* of Cl-RB and Cl-No.30 with identical nucleotide sequence (linker and FLAG-tag coding sequence).

For virus detection by RT-PCR, we used primer set no.3735/no.3736 for Cl-I89-1 and Cl-90-1 Br2, and no.3908/no.3909 for BY-CS. PCR was done using KOD-FX DNA polymerase (TOYOBO) according to the manufacturer's instructions.

Sequences of the primers are available upon request.

Agrobacterium-mediated transient expression

Agrobacterium-mediated transient expression was conducted as described previously (30). *Agrobacterium* LBA4404 cells transformed with each construct were suspended in MES buffer [10 mM 2-(*N*-morpholino)ethanesulfonic acid (MES), 10 mM $MgCl_2$, pH 5.7], and the suspensions were adjusted to OD_{600} = 1.0. Acetosyringone was added to the suspensions at a final concentration 200 μM, followed by incubation at room temperature for 2–4 h. Each suspension was infiltrated into *N. benthamiana* leaves using needleless syringes. Leaves were sprayed with 30 μM dexamethasone solution containing 0.01% Tween-20 24 h after agroinfiltration (31). Leaves were collected 24 h after dexamethasone treatment and used for western blot and real-time PCR analysis.

Western blot

Western blots were conducted as described previously (30, 32). Proteins were resolved in 12% NuPAGE Bis-Tris gel (Thermo Fisher Scientific) using MES-SDS buffer (FLAG-tagged protein detection) or in 10% SDS-PAGE using Tris-glycine buffer (CP detection; (33)), followed by electrotransfer to a PVDF membrane. To detect the FLAG-tagged proteins, monoclonal Anti-FLAG M2–horseradish peroxidase (HRP) (Sigma-Aldrich Corporation, St. Louis, MO) was used at a 1:5000 dilution. To detect ClYVV CP, rabbit polyclonal antibody against ClYVV CP was used as the primary antibody and alkaline-phosphatase-conjugated goat anti-rabbit IgG (Thermo Fisher Scientific) was used as the secondary antibody.

Chemiluminescence signals were detected with ECL Prime (GE Healthcare, Little Chalfont, United Kingdom) using a LAS-4000 imaging system (GE Healthcare) for FLAG-tagged protein detection, or with CDP-Star reagent (New England Biolabs, Ipswich, MA) using a LAS-4000-mini imaging system (GE Healthcare) for CP detection. As a loading control for the FLAG-tagged protein experiment, membranes after transfer were stained with 0.1% amido black in 45% methanol and 10% acetic acid followed by destaining in 90% methanol and 2% acetic acid (34).

GFP fluorescence analysis

GFP fluorescence of pea plants infected with GFP-tagged viruses (Cl-No.30/GFP and Cl-RB/GFP) was monitored using an MVX10 epifluorescence microscope (Olympus Corporation, Tokyo, Japan). The fluorescent area was measured by using the color thresholding tool of ImageJ software (35).

Double-antibody sandwich enzyme-linked immunosorbent assay (DAS-ELISA)

DAS-ELISA was conducted according to our previous report (32). A single GFP focus derived from virus was excised from inoculated leaves and used for antigens. We used a mouse anti-ClYVV CP IgG as the first antibody and rabbit anti-ClYVV CP as the second antibody. After washing, alkaline-phosphatase-conjugated goat anti-rabbit IgG was added, followed by the substrate solution (disodium ϱ-nitrophenyl-phosphate hexahydrate in 10% diethanolamine). The intensity of the signal was measured at an optical density (OD) of 405 nm.

Determination of full-length ORF sequence of Cl-I89-1

cDNA was synthesized from total RNA isolated from pea leaves infected with Cl-I89-1. The sequence covering the full-length Cl-I89-1 ORF was amplified using high-fidelity DNA polymerase (KOD-plus2 neo; TOYOBO) into four overlapping fragments using the following primer sets: no.3230/no.3191, no.2978/no.2493, no.2388/no.2471, and no.2470/no.3229. The four PCR products were directly sequenced by the primer-walking method using primers no.157, no.2372, no.2451, no.2464, no.2470, no.2481, no.2491, no.2552, no.2559, no.2621, no.3130, no.3436, and no.3435. The GenBank/ENA/DDBJ accession number for the full-length ORF sequence of Cl-I89-1 is LC096082. Sequences of the primers are available upon request.

Phylogenetic analysis

Phylogenetic analysis was performed for full-length nucleotide sequences encoding polyprotein of ClYVV and BYMV. Sequence alignment was conducted using MUSCLE, and a maximum-likelihood tree was inferred using the MEGA6 package (36). The nucleotide substitution models and rates among sites were general time-reversible and gamma distribution. The significance of the nodes was estimated with 1000 bootstrap replicates.

RESULTS

P3 of Cl-90-1 Br2 was the major virulence determinant in PI 226564

Cl-90-1 Br2 induced lethal systemic cell death in PI 226564 (Fig. 1A, Table 1). To identify the virulence determinant of Cl-90-1 Br2 in PI 226564, chimeric viruses were constructed by swapping parts of Cl-90-1 Br2 and Cl-No.30; the latter virus does not induce cell death in PI 226564 (Fig. 1A, Table 1) (20, 21). These chimeric viruses were based on Cl-No.30 infectious cDNA that we previously constructed and developed for use as a gene expression vector (7, 23, 37, 38). Chimeric viruses tagged with GFP were created that covered almost all

327 regions of the ClYVV genome: Cl-P1HC/GFP, Cl-BB/GFP, Cl-NS/GFP, and Cl-SB/GFP
328 (Fig. 1B) (7). Symptoms indicated that only the BB region of Cl-90-1 Br2 markedly
329 enhanced the virulence of Cl-No.30 (Fig. 1C). Cl-BB/GFP induced cell death in upper
330 uninoculated leaves (Fig. 1C). The P1HC and SB regions of Cl-90-1 Br2 did not enhance Cl-
331 No.30 virulence (Fig. 1C). The NS region slightly enhanced the virulence: Cl-NS/GFP
332 occasionally induced cell death associated with yellowing in upper uninoculated leaves (Fig.
333 1C). In contrast to Cl-90-1 Br2, Cl-BB/GFP did not kill completely the plants, but a mosaic
334 pattern associated with cell death developed in the upper uninoculated leaves (Fig. 1C).
335 Further analysis was focused on the virulence enhancement mediated by the Cl-90-
336 1 Br2 BB region, which included ca. 94% of *HC-Pro* and ca. 79% of *P3* from Cl-90-1 Br2.
337 Cl-P1HC/GFP had the full-length *HC-Pro* gene of Cl-90-1 Br2 but could not enhance
338 virulence (Fig. 1B and C), suggesting that the *P3*-containing portion of the BB region
339 (designated P3B as shown in Fig. 1B) was important for high virulence expression. We
340 constructed Cl-RB/GFP, in which the P3B region of Cl-No.30 was replaced by that of Cl-90-
341 1 Br2 (Fig. 1B). Cl-RB/GFP extensively induced cell death in upper uninoculated leaves,
342 comparable to that induced by Cl-BB/GFP (Fig. 1C).
343 Like Cl-BB/GFP, Cl-RB/GFP did not kill the plants. To investigate whether
344 insertion of *GFP* (which was present in the first set of chimeric constructs tested) attenuated
345 ClYVV virulence, the symptoms induced by Cl-No.30 with *GFP* (inserted between *P1* and
346 *HC-Pro* or between *NIb* and *CP*) were compared with those induced by Cl-No.30 without
347 *GFP*. The results indicated that insertion of *GFP* weakened the symptoms produced by
348 ClYVV (Fig. D), although virus accumulation was not visibly different as measured by
349 western blotting against CP (Fig. D). To investigate whether the weaker virulence of Cl-
350 RB/GFP relative to Cl-90-1 Br2 was due to *GFP* insertion, we compared the virulence of Cl-
351 RB without *GFP* with that of Cl-90-1 Br2 (7) and Cl-No.30 without *GFP* (37). Cl-RB

without *GFP* also induced more severe symptoms than Cl-No.30 without *GFP*, but did not have the level of virulence of Cl-90-1 Br2 (Fig. 1E). We also examined the reciprocal chimera of Cl-RB, Cl-90-1 Br2-P3B$^{No.30}$ without *GFP*, which contained the P3B region from Cl-No.30 and all other regions from Cl-90-1 Br2 (Fig. 1B). Cl-90-1 Br2-P3B$^{No.30}$ without *GFP* induced yellowing and cell death in upper uninoculated leaves, but the timing was delayed in comparison with Cl-RB without *GFP* (Fig. 1F). It indicated that Cl-90-1 Br2-P3B$^{No.30}$ showed less virulence than Cl-RB, and more virulence than Cl-No.30. Together, these results indicated that the P3B region was the main determinant of virulence in PI 226564, though regions outside of P3B also contributed to virulence expression.

To identify the virulence determinant(s) outside the P3B region, we created chimeric viruses without *GFP* each of which has P1HC, NS, or SB regions of Cl-90-1 Br2 in addition to P3B of Cl-90-1 Br2, so that almost all regions of the ClYVV genome were covered (Fig. 1B). All of the chimeric viruses expressed higher virulence than Cl-RB at 21 days post inoculation (dpi) (Fig. 1G); they induced cell death in both inoculated and upper uninoculated leaves. Plants infected with Cl-RB+P1HC, Cl-RB+NS, or Cl-RB+SB were shorter than those infected with Cl-RB; however, none of the chimeric viruses killed the plants completely (Fig. 1G).

Taken together, these data showed that Cl-No.30 carrying Cl-90-1 Br2 regions outside of P3B (Cl-P1HC, Cl-NS, Cl-SB, and Cl-90-1 Br2-P3B$^{No.30}$) had weaker virulence than Cl-No.30 carrying the P3B region of Cl-90-1 Br2 (Cl-RB) and those in combination with Cl-90-1 Br2 regions (Cl-RB+P1HC, Cl-RB+NS, Cl-RB+SB). This indicated that the effect of virulence was the highest in exchanging the P3B region and the effect of virulence enhancement by regions outside of P3B was higher in virus carrying the P3B region of Cl-90-1 Br2 than in virus carrying the P3B region of Cl-No.30. These symptom observations collectively suggested that, although regions outside of *P3* contributed to virulence

expression, the *P3* gene (P3B region) was the major determinant for inducing lethal systemic cell death in PI 226564.

P3N-PIPO, but not P3, of Cl-RB was responsible for cell death induction in PI 226564

P3 expresses two mature proteins, P3 and P3N-PIPO (8). To dissect which protein induces cell death, *P3*, *P3ΔPIPO*, and *P3N-PIPO* from Cl-RB were expressed in PI 226564 by WClMV vectors (designated WCl/P3-RB, WCl/P3ΔPIPO-RB, and WCl/P3N-PIPO-RB, respectively) (24). We have previously shown that WClMV can infect PI 226564 but does not induce cell death (25) (Table 1). The *P3* construct was expected to produce P3 protein accompanied by a small amount of P3N-PIPO protein as a frameshift product (Fig. 2A) (24). *P3ΔPIPO* had a mutation enabling it to produce P3 but not P3N-PIPO (Fig. 2A) (24). *P3N-PIPO* had mutations enabling it to express P3N-PIPO in the zero frame but not P3 frame product (Fig. 2A) (24). We inoculated PI 226564 with the three WClMV vectors and WClMV expressing *GFP* (WCl/GFP) as a negative control.

We found that WCl/P3N-PIPO-RB extensively induced cell death along the veins of inoculated leaves at 5 dpi (Fig. 2B, Table 1). In contrast, infection with WCl/P3-RB, WCl/P3ΔPIPO-RB, and WCl/GFP did not induce cell death (Fig. 2B). These results suggested that P3N-PIPO, not P3, was the factor responsible for inducing cell death in PI 226564. It should be noted that the nucleotide sequence of *P3N-PIPO* of Cl-RB is the same as that of Cl-90-1 Br2.

P3N-PIPO of Cl-No.30 also induced cell death in PI 226564

Cl-No.30 does not induce cell death in PI 226564, which suggested that P3N-PIPO of Cl-No.30 would not induce cell death either (20). We inoculated PI 226564 with WClMV carrying *P3N-PIPO*, *P3*, or *P3ΔPIPO* of Cl-No.30 (designated WCl/P3-No.30,

WCl/P3ΔPIPO-No.30, and WCl/P3N-PIPO-No.30, respectively). Unexpectedly, WCl/P3N-PIPO-No.30 extensively induced cell death along the veins on the inoculated leaves in PI 226564 (Fig. 2C, Table 1). This symptom was comparable to that induced by WCl/P3N-PIPO-RB (Fig. 2B). WCl/P3-No.30, WCl/P3ΔPIPO-No.30, and WCl/GFP did not induce cell death at 5 dpi in PI 226564 (Fig. 2C).

We constructed a WClMV vector that expresses *P3N-PIPO* from the BYMV CS strain (BY-CS), designated WCl/P3N-PIPO-CS, in order to rule out the possibility that cell death was non-specifically caused by overexpression of *P3N-PIPO*. We expected that P3N-PIPO of BY-CS would not induce cell death because BY-CS has never been reported to induce cell death in pea, including PI 226564 (20, 21). Like ClYVV, however, BY-CS is a member of genus *Potyvirus*, and the two are closely related (39). The nucleotide sequence identity of *P3N-PIPO* between BY-CS and Cl-90-1 Br2 or Cl-No.30 is 64.2% or 61.9%, respectively. The amino acid sequence identity (similarity) of P3N-PIPO between BY-CS and Cl-90-1 Br2 or Cl-No.30 is 56.5% (73.8%) or 54.9% (71.3%), respectively (Fig. 3). In PI 226564 infected with WCl/P3N-PIPO-CS, cell death was not induced in either inoculated or upper uninoculated leaves even at 14 dpi (Fig. 2D, Table 1), thus ruling out the possibility that overexpression of *P3N-PIPO* non-specifically induced cell death.

P3N-PIPO of Cl-No.30 and RB, but not of BY-CS, activated the SA signaling pathway in PI 226564

One of the possible mechanisms that induces cell death by P3N-PIPO is high activation of the SA signaling pathway. We previously showed that activation of the SA signaling pathway contributes to induction of systemic cell death by ClYVV in susceptible peas PI 118501 and PI 226564 (20). Therefore, we hypothesized that expression of Cl-90-1 Br2 P3N-PIPO

426 activated the SA signaling pathway, which led to induction of systemic cell death in PI
427 226564.

428 To test this hypothesis, we analyzed the expression of SA-responsive chitinase gene
429 (*SA-CHI*) and an HR-related gene homologous to tobacco *HSR203J* (*HSR203J*) by real-time
430 PCR. We conducted an expression analysis in leaves of PI 226564 inoculated with Cl-90-1
431 Br2, Cl-No.30, or BY-CS. The expression level of *SA-CHI* was significantly higher in leaves
432 inoculated with Cl-90-1 Br2 than in leaves inoculated with either Cl-No.30 or BY-CS (Fig.
433 4A). There were no significant differences among mock, Cl-No.30, and BY-CS inoculation
434 (Fig. 4A). The expression level of *HSR203J* was also significantly higher in the leaves
435 inoculated with Cl-90-1 Br2 than in those with mock inoculation (Fig. 4B). These results
436 indicated that Cl-90-1 Br2 infection activated SA and HR-like signaling pathways in PI
437 226564.

438 We carried out an expression analysis of *SA-CHI* in leaves of PI 226564 inoculated
439 with WCl/P3N-PIPO, WCl/P3, or WCl/P3ΔPIPO from Cl-RB; the corresponding set of
440 sequences from Cl-No.30; or WCl/GFP. At 4 dpi, *SA-CHI* was significantly induced only in
441 leaves inoculated with WCl/P3N-PIPO-RB or WCl/P3N-PIPO-No.30 (Fig. 4C and D).
442 WCl/P3 and WCl/P3ΔPIPO (from both Cl-RB and Cl-No.30), GFP, and mock inoculations
443 did not significantly induce *SA-CHI* (Fig. 4C and D). We also investigated the expression
444 level of *SA-CHI* in the leaves inoculated with WCl/P3N-PIPO-CS (from BY-CS) and
445 confirmed that WCl/P3N-PIPO-CS infection did not induce *SA-CHI* expression (Fig. 4D).
446 The amplitudes of *SA-CHI* upregulation in plants infected with WCl/P3N-PIPO of Cl-RB and
447 Cl-No.30 (Fig. 4C and D) were several orders of magnitude higher than those in plants
448 infected with Cl-RB (Fig. 4A), possibly because Cl-RB produced lower levels of P3N-PIPO
449 (produced by transcriptional slippage) than did WClMV carrying *P3N-PIPO* (produced in
450 zero frame).

Lower accumulation of Cl-No.30 P3N-PIPO than Cl-RB P3N-PIPO was presumably the reason for the lower virulence of Cl-No.30

We found that heterologous expression of Cl-No.30 P3N-PIPO could induce cell death in PI 226564 (Fig. 2C, Table 1), which was seemingly inconsistent with the fact that Cl-No.30 does not induce cell death in this same cultivar (Fig. 1A, Table 1) (20, 21). We previously showed that P3N-PIPO could be detected in Cl-RB-infected plants but was below the level of detection in Cl-No.30-infected plants of a susceptible pea cultivar, PI 250438, indicating that the level of P3N-PIPO from Cl-No.30 is significantly lower than that from Cl-90-1 Br2 (7). This same difference was observed when P3N-PIPO was produced from the *P3* cistron of each virus using an *in vitro* translation system with an *A. thaliana* cell-free system and wheat germ extract (7, 13). In this study, we compared the accumulation of Cl-No.30 P3N-PIPO and Cl-RB P3N-PIPO in a transient expression system, agroinfiltration in *N. benthamiana* leaf tissues.

We prepared construct *P3(PIPO:FLAG^{-1})*, in which a *FLAG* epitope tag sequence was inserted in front of the stop codon of the *PIPO* coding sequence, as a means to detect PIPO-frame products (Fig. 5A) (13). *P3(PIPO:FLAG^{-1})* constructs of Cl-RB and Cl-No.30 were transiently expressed in the same leaf of *N. benthamiana*, and the production of protein from the PIPO frame and mRNA of *P3(PIPO:FLAG^{-1})* was compared by measuring the protein/mRNA ratio. Western blotting using a FLAG antibody indicated that the accumulation of PIPO-frame products of Cl-RB was higher than that of Cl-No.30 in three independent plants (Fig. 5B). Similar results were observed in at least three independent experiments. In contrast, real-time PCR analysis indicated that mRNA level of Cl-No.30 *P3(PIPO:FLAG^{-1})* was higher than that of Cl-RB (Fig. 5C). Thus, the protein/mRNA ratio of Cl-No.30 was significantly lower than that of Cl-RB (Fig. 5D). As a control experiment, we

476 compared the protein/mRNA ratio of *P3N-PIPO:FLAG*^{mk}, which has mutations that enable
477 production of *P3N-PIPO* mRNA in the zero frame but does not produce *P3* mRNA, between
478 Cl-RB and Cl-No.30 (Fig. 5A) (13). Western blot analysis indicated that there were no visible
479 differences in protein accumulation between Cl-RB and Cl-No.30 (Fig. 5E). Real-time PCR
480 analysis indicated that the mRNA level of Cl-No.30 *P3N-PIPO:FLAG*^{mk} tended to be higher
481 than that of Cl-RB (Fig. 5F). Thus, the protein/mRNA ratio of Cl-No.30 was lower than that
482 of Cl-RB (Fig. 5G). These results showed that P3N-PIPO production from *P3* cistron of Cl-
483 No.30 was lower than that from *P3* cistron of Cl-RB in a transient expression in *N.*
484 *benthamiana* leaf tissues.

485 We also obtained data supporting the possibility that the increased levels of P3N-
486 PIPO produced by Cl-RB enhance virus accumulation in infected plants. We compared the
487 accumulation of Cl-RB with that of Cl-No.30 by using GFP-tagged versions of each virus.
488 P3N-PIPO is an essential factor for potyviruses to move cell-to-cell in infected leaves (40).
489 Therefore, we anticipated that Cl-RB would accumulate more efficiently than Cl-No.30 in PI
490 226564 if the level of Cl-RB P3N-PIPO was higher than that of Cl-No.30 P3N-PIPO. Virus
491 accumulation levels were compared between Cl-No.30/GFP and Cl-RB/GFP in PI 226564.
492 We excised infection foci (GFP-expressing areas) from inoculated leaves using an
493 epifluorescence microscope (Fig. 6A) and measured the CP amount of each virus by DAS-
494 ELISA (Fig. 6B). The result showed that Cl-RB/GFP accumulated to higher levels than Cl-
495 No.30/GFP at 5 dpi. By measuring the GFP-fluorescent area, we also found that Cl-RB/GFP
496 spread more rapidly than Cl-No.30/GFP at 5 dpi (Fig. 6C). These results suggested that
497 higher production of P3N-PIPO enhanced the ability of Cl-RB to accumulate in the infected
498 pea, perhaps synergistically increasing the difference in accumulation of P3N-PIPO between
499 pea plants infected with Cl-RB and Cl-No.30.

These results collectively suggest that the lower level of Cl-No.30 P3N-PIPO enabled Cl-No.30 to avoid activating the SA signaling pathway, resulting in the loss of cell death induction in PI 226564.

The increased virulence in Cl-90-1 Br2 relative to Cl-90-1 appears to be caused by a single amino acid difference in P3N-PIPO (P3)

Cl-90-1 Br2, a mutant isolate that originated from Cl-90-1, expressed higher virulence than Cl-90-1, which induced cell death in upper uninoculated leaves of PI 226564 but did not kill the plants (Fig. 7, Table 1). We anticipated that the P3B region was responsible for the virulence enhancement in Cl-90-1 Br2 relative to Cl-90-1. We created a chimeric virus based on Cl-RB/GFP with the P3B region (from Cl-90-1 Br2) replaced by that of Cl-90-1 (Fig. 7A). There is a single non-synonymous difference between the two sequences (T [Cl-90-1 Br2] vs. G [Cl-90-1]) that causes a substitution of methionine (Cl-90-1 Br2) with arginine (Cl-90-1) at amino acid position 28 of P3 (Fig. 7B); thus, the chimeric virus was designated as Cl-RB^{M28R}/GFP. As expected, the symptoms induced by Cl-RB^{M28R}/GFP were weaker than those induced by Cl-RB/GFP (Fig. 7C and D). Cl-RB^{M28R}/GFP induced yellowing and cell death in upper uninoculated leaves, but the timing was delayed in comparison with Cl-RB/GFP (Fig. 7D). The plants infected with Cl-RB^{M28R}/GFP were reproducibly taller than those infected with Cl-RB/GFP (Fig. 7C). The substitution at aa position 28 of P3N-PIPO (P3) is in the N-terminal region, distant from the PIPO coding region (Fig. 3), suggesting that the substitution did not affect PIPO-frame translation and qualitatively affected virulence through some other mechanism. It should be noted that Cl-RB/GFP can break *cyv1* resistance whereas Cl-RB^{M28R}/GFP cannot, indicating that the same single amino acid substitution affected both breaking of *cyv1* recessive resistance and symptom severity in susceptible cultivar PI 226564

524 (7). The substitution at aa position 28 is also close to the position important for PSbMV
525 virulence in pea carrying *sbm-2* recessive resistance (Fig. 3) (41).
526
527 **P3N-PIPO also induced cell death in two other pea lines, PI 118501 and PI 429853.**
528 To investigate whether the P3N-PIPO proteins of Cl-90-1 Br2, Cl-No.30, and BY-CS had the
529 ability to induce cell death in PI 118501 (*Cyn1*) (21) and PI 429853 (*cyv1*) (7), these P3N-
530 PIPO proteins were expressed by WClMV vectors in these two lines. P3N-PIPO of Cl-90-1
531 Br2 and Cl-No.30 extensively induced cell death at 5 dpi in PI 118501, whereas P3N-PIPO of
532 BY-CS did not induce cell death until 8 dpi (Fig. 8A, Table 1). The same pattern was
533 observed for infection of PI 429853 (Fig. 8B and C, Table 1). These results indicated that
534 each P3N-PIPO protein had the ability to induce cell death in both PI 118501 and PI 429853.
535 The results were inconsistent with symptoms in the context of virus infection (Table 1),
536 suggesting that cell death induction was determined by other factors in addition to P3N-PIPO.
537
538 **Cell death induction was not determined solely by the PIPO region**
539 In PI 226564, P3N-PIPO of Cl-RB induced cell death but P3 did not (Fig. 2B). As P3N-PIPO
540 has the same N-terminal region (P3N) as P3, PIPO is the only region distinguishing P3N-
541 PIPO from P3. Therefore, we inferred that the PIPO domain of Cl-RB was responsible for
542 cell death induction in PI 226564. To test this possibility, we created chimeric *P3N-PIPO*
543 genes that had either *P3N* of Cl-RB and *PIPO* of BY-CS ($P3N^{RB}$-$PIPO^{CS}$) or *P3N* of BY-CS
544 and *PIP*O of Cl-RB ($P3N^{CS}$-$PIPO^{RB}$); these combinations were chosen because P3N-PIPO of
545 BY-CS did not induce cell death in PI 226564 (Fig. 2D). $P3N^{RB}$-$PIPO^{CS}$ and $P3N^{CS}$-$PIPO^{RB}$
546 were expressed by WClMV vectors in PI 226564. $P3N^{CS}$-$PIPO^{RB}$ expression induced cell
547 death in the inoculated leaves, but it was markedly weaker than that induced by P3N-PIPO of
548 Cl-RB (Fig. 9A). $P3N^{RB}$-$PIPO^{CS}$ expression did not induce cell death (Fig. 9A).

549 We also expressed the chimeric P3N-PIPO proteins in PI 118501 by using the same
550 WClMV vectors. When we inoculated PI 118501 with WCl/P3N^{RB}-PIPO^{CS} or WCl/P3N^{CS}-
551 PIPO^{RB}, neither one induced cell death at 5 dpi or even at 18 dpi in the inoculated leaves,
552 although both WCl/P3N-PIPO-RB and WCl/P3N-PIPO-CS induced severe cell death at 18
553 dpi (Fig. 9B).
554
555 **A consistent gradation of virulence was observed among ClYVV isolates in *cyv1* and**
556 **susceptible peas**
557 Previous studies using PI 429853 (*cyv1*) indicated that Cl-No.30 never infects this line, Cl-
558 90-1 can produce resistance-breaking mutants, and Cl-90-1 Br2 and Cl-I89-1 can
559 systemically infect this line (Table 1) (7). In this study, we compared the symptoms between
560 Cl-90-1 Br2 and Cl-I89-1. Cl-90-1 Br2 induced no symptoms in PI 429853 (*cyv1*), whereas
561 Cl-I89-1 induced chlorosis and cell death systemically at 25 dpi (Fig. 10A). RT-PCR analysis
562 of upper uninoculated leaves confirmed Cl-I89-1 infection in all three plants and confirmed
563 Cl-90-1 Br2 infection in two out of three plants (Fig. 10A and B). Plants inoculated with BY-
564 CS did not show any symptoms at 25 dpi in PI 429853 (*cyv1*), and RT-PCR analysis
565 indicated that no plants were infected with BY-CS (Fig. 10C). Therefore, the order of
566 virulence in PI 429853 (*cyv1*) was Cl-I89-1 > Cl-90-1 Br2 > Cl-90-1 > Cl-No.30 and BY-CS
567 (Table 1). Similarly, the symptom severity in susceptible pea line PI 226564 was Cl-90-1 Br2
568 > Cl-90-1 > Cl-No.30 (Fig. 7, Table 1) (20, 42). We compared the symptom severities
569 between Cl-I89-1 and Cl-90-1 Br2, and between Cl-No.30 and BY-CS. The symptoms
570 induced by Cl-I89-1 were more severe than those induced by Cl-90-1 Br2 at 10 dpi in PI
571 226564 (Fig. 10D). The symptoms induced by Cl-No.30 were more severe than those
572 induced by BY-CS at 10 dpi in PI 226564 (Fig. 10E) These results indicated a consistent

573 gradation of virulence among these viruses in both PI 429853 (*cyv1*) and susceptible PI
574 226564 (Table 1).

575 Next, we investigated whether the same gradation was observed in another
576 susceptible cultivar, PI 118501, which shows lethal systemic cell death following Cl-No.30
577 infection but not BY-CS infection (20, 21). The inoculation test indicated that Cl-I89-1, Cl-
578 90-1 Br2, Cl-90-1, and Cl-No.30 similarly induced lethal systemic cell death (Fig. 10F),
579 whereas BY-CS induced only mosaic symptoms in the upper uninoculated leaves at 12 dpi
580 (Fig. 10G and H). Cell death induction by Cl-No.30 was slightly slower than induction by Cl-
581 I89-1, Cl-90-1 Br2, and Cl-90-1. These results indicated that the order of symptom severity in
582 PI 118501 was Cl-I89-1, Cl-90-1 Br2 and Cl-90-1 > Cl-No.30 > BY-CS (Table 1). Taken
583 together, these results indicated that a consistent gradation exists in virulence among ClYVVs
584 and BYMV in PI 429853 (*cyv1* recessive resistance) and in PI 226564 and PI 118501
585 (susceptible) (Table 1; Fig. 10I).

586 Phylogenetic analysis using full-length ORF sequences encoding polyprotein
587 suggested that high-virulence isolates (Cl-90-1, Cl-90-1 Br2, and Cl-I89-1) form a group
588 distinct from the low-virulence isolate Cl-No.30 (Fig. 10J).

589

590 **DISCUSSION**

591 We revealed that the main determinant of lethal systemic cell death induction by ClYVV was
592 P3N-PIPO. This was determined by analysis using chimeric viruses and transient expression
593 from WClMV vectors in a susceptible pea cultivar, PI 226564. SMV strain G7 induces lethal
594 systemic cell death in soybean carrying the dominant resistance gene *Rsv1* (14). In that virus,
595 *P3*, not *P3N-PIPO*, determines virulence (40). TuMV induces lethal systemic cell death in *A.*
596 *thaliana* L*er* carrying the *TuNI* gene (15). TuMV *P3* expression alone is sufficient for
597 induction of cell death at a single-cell level, and the region required for cell death induction is

598 upstream of the *PIPO* coding sequence (43). Our study is the first report to suggest that
599 induction of lethal systemic cell death could be attributed to P3N-PIPO.

600 As mentioned above, it was unexpected to see that expression of P3N-PIPO from
601 Cl-No.30 by a WClMV vector induced cell death in PI 226564 (Fig. 2C) because Cl-No.30
602 itself does not induce cell death in this cultivar (Fig. 1A) (20, 21). In *N. benthamiana*, the
603 *Plantago asiatica* mosaic virus (PlAMV) Li1 isolate induces systemic necrosis that has HR-
604 like characteristics (44, 45). Transient expression of the PlAMV Li1 isolate RdRp (helicase
605 domain) by agroinfiltration induces cell death in *N. benthamiana* (46). These results suggest
606 that *N. benthamiana* recognizes PlAMV RdRp and induces an HR-like response systemically,
607 resulting in systemic necrosis. Interestingly, transient expression of RdRp encoded by the
608 PlAMV Li6 asymptomatic isolate also induces cell death in *N. benthamiana* (46). RdRp
609 accumulation is higher in the areas infiltrated with *Agrobacterium* carrying infectious cDNA
610 of the Li1 isolate than when infectious cDNA of the Li6 isolate is used (46). These results
611 suggest that *N. benthamiana* has the ability to recognize both Li1 and Li6 RdRp, but the
612 difference in their protein accumulation levels determines the induction of systemic necrosis
613 in the context of virus infection. The results reported here can be explained in a similar
614 fashion. Previously, we reported that in susceptible pea PI 250438 infected with Cl-90-1 Br2
615 or Cl-No.30, the P3N-PIPO of Cl-90-1 Br2 could be detected but that Cl-No.30 was below
616 the level of detection when tested using an antibody against the PIPO peptide (7).
617 Furthermore, we showed that the amount of P3N-PIPO produced from the *P3* cistron of Cl-
618 No.30 is significantly less than that of Cl-RB in an *in vitro* translation system using MM2dL
619 (an extract derived from *A. thaliana* MM2d cells) and wheat germ extract (7, 13). In this
620 study, we showed evidence that the *P3* cistron of Cl-No.30 produced less P3N-PIPO protein
621 than that of Cl-RB *in vivo* in agroinfiltrated *N. benthamiana* (Fig. 5B). The protein/mRNA
622 ratio of Cl-No.30 was lower than that of Cl-RB (Fig. 5D). These results suggest that P3N-

623 PIPO production, or transcriptional slippage efficiency, from Cl-No.30 *P3(PIPO:FLAG^{-1})*
624 (which tagged P3N-PIPO produced by frameshift) is lower than that from Cl-RB. On the
625 other hand, the protein/mRNA ratio of Cl-No.30 *P3N-PIPO:FLAG^{mk}* (which produced tagged
626 P3N-PIPO as a zero-frame product) was also lower than that of Cl-RB (Fig. 5G). The
627 protein/mRNA ratio of *P3(PIPO:FLAG^{-1})* tended to be lower than that of *P3N-*
628 *PIPO:FLAG^{mk}* in repeated experiments, though there was not a statistically significant
629 difference. These findings suggest that the difference in P3N-PIPO accumulation between Cl-
630 No.30 and Cl-RB was determined by a combination of transcriptional slippage efficiency and
631 other factors such as protein stability or translation efficiency. Taken together, these results
632 support the hypothesis that in susceptible pea PI 226564, Cl-90-1 Br2 can produce P3N-PIPO
633 protein sufficient for induction of cell death but Cl-No.30 cannot, even though host cells are
634 able to recognize P3N-PIPO from both isolates.

635 We showed that each of the tested regions outside of *P3* are accessorily involved in
636 the virulence enhancement in PI 226564 (Fig. 1G). In previous studies, we revealed that the
637 *HC-Pro* gene is indirectly involved in the induction of lethal systemic cell death in PI 118501
638 (20, 22, 32). We found that a Cl-No.30 mutant with a D to Y substitution in amino acid
639 position 193 of HC-Pro (Cl-D193Y) loses the ability to induce cell death in PI 118501 (20).
640 Potyvirus HC-Pro is an RNA-silencing suppressor required for efficient virus accumulation
641 in host plants (47). The D193Y mutation in HC-Pro markedly reduces its ability to suppress
642 RNA silencing, and Cl-D193Y accumulation is significantly lower than wild-type Cl-No.30
643 in PI 118501 (20, 22). Heterologous expression of viral suppressors of RNA silencing
644 (tomato bushy stunt virus P19 or cucumber mosaic virus 2b) can complement the virulence of
645 Cl-D193Y in PI 118501 (32). These results suggest that HC-Pro itself is not an elicitor but
646 indirectly affects cell death induction via its RNA-silencing suppressor activity in PI 118501:
647 reduced accumulation of ClYVV leads to reduced accumulation of the elicitor molecules that

induce cell death. In this study, we found that the elicitor molecule active against PI 118501 was P3N-PIPO (Fig. 8A). Thus, is likely that Cl-D193Y is not lethal in PI 118501 because it cannot produce enough P3N-PIPO to induce cell death. Taken together, the results indicate that lethal systemic cell death in PI 118501 was induced by P3N-PIPO, the production of which was indirectly regulated by the RNA-silencing suppressor activity of HC-Pro. As observed for *HC-Pro*, viral genes other than *P3* might increase the accumulation of P3N-PIPO, enhancing the virulence in PI 226564 (Fig. 1G).

We found that expression of *P3N-PIPO* from Cl-90-1 Br2, Cl-No.30, and BY-CS by WClMV vectors induced cell death in PI 226564, PI 118501, and PI 429853, with the exception of BY-CS *P3N-PIPO* in PI 226564 (Table 1), suggesting that many peas have a common factor that recognizes P3N-PIPO of two different *Potyvirus* species (ClYVV and BYMV). The *Rx* gene in potato encodes an NB-LRR–type resistance gene that confers genetically dominant resistance against potato virus X (PVX) (48). Rx specifically recognizes CP of PVX avirulent strains and induces extreme resistance (epistatic to HR) (49). *N. benthamiana* expressing *Rx* also shows resistance to PVX (50). Interestingly, Rx is able to recognize CP of three other species in the genus *Potexvirus* (narcissus mosaic virus, WClMV, and cymbidium mosaic virus) and to induce HR in *N. benthamiana* expressing *Rx* (51). The product of the L^4 resistance gene (NB-LRR) isolated from pepper is able to recognize CP of several distant species in the genus *Tobamovirus* including tomato mosaic virus, TMV, paprika mild mottle virus, and pepper mild mottle virus, and to induce cell death accompanied by HR when both *CP* and L^4 are transiently expressed in *N. benthamiana* by agroinfiltration (34). Similarly, the product of *N'* (NB-LRR) isolated from *Nicotiana sylvestris* is able to recognize CP of tomato mosaic virus, paprika mild mottle virus, and pepper mild mottle virus and induces cell death accompanied by HR when both *CP* and *N'* are transiently expressed in *N. benthamiana* by agroinfiltration (34). These studies suggest

673 that a single resistance protein has the potential to recognize a wide range of elicitor
674 molecules, at least within the same genus.

675 In pea, one of the candidate factors to recognize P3N-PIPO is the product of the
676 *Cyn1* gene (21). Genetic analysis indicated that the lethal systemic cell death induced by Cl-
677 No.30 in PI 118501 is controlled by the dominant gene *Cyn1* (21). *Cyn1* is located on linkage
678 group (LG) 3, where many *R* gene analogs were suggested to be clustered by a synteny study
679 between pea and *Medicago truncatula* (21). In this study, we showed that expression of *P3N-*
680 *PIPO* of Cl-No.30 in a WClMV vector induced cell death in PI 118501 (Fig. 8A), suggesting
681 that Cyn1 recognized P3N-PIPO and induced lethal systemic cell death. We previously
682 showed the possibility that PI 226564 also has a *Cyn1* allele that weakly recognizes Cl-No.30
683 (20). Cl-No.30 does not induce cell death in PI 226564 (Fig. 1A) (20, 21); however,
684 activation of the SA signaling pathway by application of an SA analog, benzo (1,2,3)
685 thiadiazole-7-carbothioic acid *S*-methyl ester (BTH), induces systemic cell death in PI
686 226564 infected with Cl-No.30 (20). In this study, we obtained the supporting result that
687 expression of Cl-No.30 *P3N-PIPO* by a WClMV vector induced cell death in PI 226564 (Fig.
688 2C). In contrast, BTH treatment does not induce cell death in PI 226564 infected with BY-CS
689 (20). Consistent with this result, expression of BY-CS *P3N-PIPO* by WClMV did not induce
690 cell death in PI 226564 (Fig. 2D). These results suggest that PI 226564 has a *Cyn1* allele
691 whose product has the potential to specifically recognize Cl-No.30 but not BY-CS. Cyn1 of
692 PI 226564 might be able to recognize P3N-PIPO effectively when P3N-PIPO is accumulated
693 to high levels, e.g., in situations such as overexpression by a WClMV vector or Cl-RB
694 infection, but not when it is at low levels, e.g., in a situation such as Cl-No.30 infection (20).
695 In PI 429853 (*cyv1*), P3N-PIPO protein could be recognized when expressed by a WClMV
696 vector, suggesting that PI 429853 has a *Cyn1* allele whose product recognizes ClYVV. It was
697 inconsistent with symptoms in the context of virus infection (Table 1). The *cyv1*-mediated

698 resistance would inhibit or reduce accumulation of ClYVV and thus the recognition of P3N-
699 PIPO under natural infection conditions (Table 1). In contrast to its lack of effect in PI
700 226564, P3N-PIPO of BY-CS could induce cell death in PI 118501 and PI 429853, though
701 more slowly than P3N-PIPO of either Cl-90-1 Br2 or Cl-No.30 (Figs. 2 and 8); these data
702 suggest that Cyn1 of PI 118501 and PI 429853 can recognize BY-CS, although less
703 efficiently than Cl-90-1 Br2 and Cl-No.30. It is noted that we could not detect P3N-PIPO
704 expressed via WClMV vector by western blot analysis and thus could not compare the
705 accumulation levels of P3N-PIPO among the three tested pea cultivars. Taken together, these
706 results suggest that the product of *Cyn1* recognizes matching P3N-PIPO of ClYVV and
707 BYMV and activates the SA-mediated defense pathway, resulting in systemic cell death
708 induction in many peas (20).
709 We showed that expression of *P3N-PIPO* by WClMV induced cell death in PI
710 226564 but that expression of *P3* did not (Fig. 2). One possible explanation is that a pea
711 protein (e.g., the *Cyn1* product) recognizes the PIPO peptide, which is part of P3N-PIPO but
712 not P3. However, the PIPO domain of Cl-P3N-PIPO alone did not appear to induce cell death,
713 as shown in the experiment using chimeric P3N-PIPO (constructed from P3N-PIPOs of Cl-
714 RB and BY-CS) in PI 226564 (Fig. 9). Although the PIPO domain contributed to recognition
715 by peas, the overall structure of P3N-PIPO may be important for full activation of the
716 signaling pathway to induce cell death. A second possible explanation is that a pea protein
717 (e.g., the *Cyn1* product) recognizes P3N-PIPO–targeted host factor(s) (the guard/decoy
718 model) (52). Recently, it was found that PCaP1 from *A. thaliana* and its homolog NbDREPP
719 from *N. benthamiana* interact with P3N-PIPO (53, 54). PCaP1 interacts with P3N-PIPO via
720 the PIPO domain and does not interact with P3, indicating that PCaP1 is specifically targeted
721 by P3N-PIPO (53). Therefore, a pea protein may monitor the target of P3N-PIPO such as
722 PCaP1 and induce cell death. A third explanation is that pea recognizes P3N-PIPO in a

723 localization-dependent manner. Previous studies reported that P3 localizes to the ER–Golgi
724 interface and that P3N-PIPO localizes to plasmodesmata (9, 55). Therefore, P3 may not be
725 recognized due to its localization.
726 Our results using five virus isolates (four ClYVV isolates and one BYMV isolate)
727 and three pea genotypes showed that the more efficiently a particular ClYVV isolate broke
728 *cyv1* recessive resistance, the more it expressed virulence in susceptible peas carrying *Cyn1*
729 (Fig. 10I and Table 1). In particular, we observed adaptive evolution from Cl-90-1 to Cl-90-1
730 Br2, which overcame *cyv1* resistance through attaining a point mutation in the P3N domain
731 (7). This mutation also resulted in Cl-90-1 Br2 gaining higher virulence than Cl-90-1 in
732 susceptible PI 226564 (Fig. 7). Many studies have suggested that trade-offs are observed in
733 plant virus infection across hosts, and antagonistic pleiotropy (when mutations beneficial for
734 infection of one host are deleterious for infection of another one) explains such trade-offs
735 well (56, 57). For example, tobacco etch virus (TEV) infects several solanaceous plants such
736 as *N. tabacum* in nature, and some non-solanaceous plants (e.g., *Helianthus annuus* and
737 *Spinacia oleracea*) are also susceptible under experimental conditions. Analysis using a TEV
738 mutant series indicated that fitness trade-offs due to antagonistic pleiotropy are observed
739 between *N. tabacum* and non-solanaceous plants (58). Several studies suggest that viruses
740 pay a fitness cost when they overcome dominant resistance due to adaptive mutations with
741 antagonistic pleiotropic effects. In pepper, tobamoviruses that can overcome dominant
742 resistance conferred by *L* genes are less able to accumulate in susceptible plants, and virus
743 particles of breaking isolates in the soil are less stable than those of wild-type virus (59, 60).
744 In *Brassica napus*, TuMV isolates CZE1 and CDN1 are able to overcome dominant
745 resistance conferred by *TuRB01* but are outcompeted by avirulent isolate UK1 in susceptible
746 plants (61). Soybeans carrying dominant *Rsv1* or *Rsv4* alleles are resistant against SMV-N
747 (62) or three strains (SMV-N, SMV-G7, and SMV-G7d) (63), respectively. SMV-N *HC-Pro*

748 mutants or SMV *P3* mutants of the three strains can overcome these respective resistances,
749 and accumulation of these mutants is reduced in susceptible cultivars (62, 63). These studies
750 indicated that their fitness trade-offs are caused by antagonistic pleiotropy of the viral genes
751 that overcome dominant resistance. Similar observations have also been reported when
752 viruses overcome recessive resistance. Potato virus Y *VPg* double mutants show more
753 virulence than *VPg* single mutants in pepper carrying a *pvr2*^{3} recessive resistance gene (64).
754 In contrast, potato virus Y *VPg* double mutants are less virulent than single mutants in
755 susceptible pepper (64). In rice, rice yellow mottle virus mutants that can overcome *rymv1-2*
756 recessive resistance are less virulent than wild-type virus in susceptible cultivars (65).
757 These studies collectively support the hypothesis that many viruses pay fitness costs
758 to adapt to new hosts or to overcome resistances, and that these across-host trade-offs are
759 caused by adaptive mutations with antagonistic pleiotropic effects. In the case of ClYVV, our
760 results suggest that many susceptible peas carry *Cyn1*, whose product recognizes ClYVVs (or
761 their P3N-PIPO proteins, in particular) that break *cyv1* resistance. In *Cyn1* peas, these
762 ClYVVs induce an HR-like response associated with systemic cell death, resulting in plant
763 death. As noted previously, the more efficiently a particular ClYVV isolate broke *cyv1*
764 recessive resistance, the more it induced systemic cell death, resulting in a loss of tissue to
765 support virus accumulation and leading to a reduction of fitness in susceptible peas carrying
766 *Cyn1*. This observation suggests that there are fitness trade-offs between overcoming *cyv1*
767 and reducing recognition by *Cyn1* via the antagonistic pleiotropy of P3N-PIPO. The trade-
768 offs shown in previous studies (described above) involve gaining adaptation to a non-host or
769 overcoming a resistant cultivar, resulting in reduction of viral viability or virulence in a
770 susceptible host. This study is unique in terms of showing trade-offs in a virus overcoming
771 two independent defense systems in a single plant species.

We hypothesize the following model of co-evolution between ClYVV and pea, driven by the antagonistic pleiotropy of P3N-PIPO. (1) ClYVV cannot infect pea carrying the *cyv1* recessive resistance gene. (2) Selection favors mutations in the *P3* gene of ClYVV that enable P3N-PIPO to accumulate to higher levels and/or alter its protein structure, enabling the virus to overcome *cyv*1 resistance. (3) After overcoming resistance, the virus can infect and accumulate effectively, but now Cyn1 recognizes the more abundant (Cl-No.30 vs Cl-90-1 Br2) and/or adapted (Cl-90-1 vs Cl-90-1 Br2) P3N-PIPO directly or indirectly and induces cell death systemically. (4) Systemic cell death leads to loss of host viability, which is also unfavorable for the virus. (5) Selection favors mutations in ClYVV that reduce the accumulation of P3N-PIPO and/or change the amino acids of P3N-PIPO required for its recognition or function, resulting in loss of the ability to overcome *cyv1* recessive resistance. Based on the proposed model, *Cyn1* may have evolved to recognize ClYVVs (or their P3N-PIPO proteins, in particular) that break *cyv1* resistance in susceptible peas. Although *Cyn1*-mediated activation of the SA defense pathway does not appear to inhibit ClYVV infection efficiently, as observed in authentic HR (20), systemic cell death may oppose the adaptive evolution to overcome *cyv1* resistance because induction of systemic cell death leads to a loss of host viability. We assume that two independent defense mechanisms (recessive resistance and the SA defense pathway) in pea impose antagonistic pleiotropy on P3N-PIPO. Such a trade-off for virus in overcoming paired defense mechanisms may sustain the durability of resistance against fast-evolving viruses (66).

FUNDING INFORMATION

This work was supported in part by JSPS KAKENHI grant number 25850030 to G.A. and 25450055 and 16H04879 to K.S.N., the NOVARTIS Foundation Japan for the Promotion of Science (to K.S.N.), and the Asahi Glass Foundation (to K.S.N.).

ACKNOWLEDGMENTS

We thank Kazue Obara and Kami Murakami for technical assistance. We also thank Takashi Aoyama and Nam-Hai Chua for the use of binary vector pTA7001, and we thank Kappei Kobayashi and Kentaro Yoshida for critical reading of the manuscript and useful discussion.

G.A., K.S.N., and I.U. designed the research. G.A., H.S., Y.M., S.H.C., Y.H., S.R., R.S., E.J.J. J.A. and K.S.N conducted the experiments. G.A., K.S.N. and I.U. discussed the results and wrote the manuscript.

We declare that we have no conflicts of interest.

References

1. **Mandadi KK**, **Scholthof KBG**. 2013. Plant immune responses against viruses: how does a virus cause disease? Plant Cell **25**:1489–1505.
2. **Diaz-Pendon JA**, **Truniger V**, **Nieto C**, **Garcia-Mas J**, **Bendahmane A**, **Aranda MA**. 2004. Advances in understanding recessive resistance to plant viruses. Mol Plant Pathol **5**:223–233.
3. **Gibbs AJ**, **Ohshima K**, **Phillips MJ**, **Gibbs MJ**. 2008. The prehistory of potyviruses: their initial radiation was during the dawn of agriculture. PLoS ONE **3**:e2523.
4. **Robaglia C**, **Caranta C**. 2006. Translation initiation factors: a weak link in plant RNA virus infection. Trends Plant Sci **11**:40–45.
5. **Andrade M**, **Abe Y**, **Nakahara KS**, **Uyeda I**. 2009. The *cyv-2* resistance to *Clover yellow vein virus* in pea is controlled by the eukaryotic initiation factor 4E. J Gen Plant Pathol **75**:241–249.
6. **Provvidenti R**, **Hampton RO**. 1991. Chromosomal distribution of genes for resistance to seven potyviruses in *Pisum sativum*. Pisum Genet **23**:26–28.

7. **Choi SH**, **Hagiwara-Komoda Y**, **Nakahara KS**, **Atsumi G**, **Shimada R**, **Hisa Y**, **Naito S**, **Uyeda I**. 2013. Quantitative and qualitative involvement of P3N-PIPO in overcoming recessive resistance against *Clover yellow vein virus* in pea carrying the *cyv1* gene. J Virol **87**:7326–7337.

8. **Chung BYW**, **Miller WA**, **Atkins JF**, **Firth AE**. 2008. An overlapping essential gene in the Potyviridae. Proc Natl Acad Sci USA **105**:5897–5902.

9. **Wei T**, **Zhang C**, **Hong J**, **Xiong R**, **Kasschau KD**, **Zhou X**, **Carrington JC**, **Wang A**. 2010. Formation of complexes at plasmodesmata for potyvirus intercellular movement is mediated by the viral protein P3N-PIPO. PLoS Pathog **6**:e1000962.

10. **Wen RH**, **Hajimorad MR**. 2010. Mutational analysis of the putative *pipo* of soybean mosaic virus suggests disruption of PIPO protein impedes movement. Virology **400**:1–7.

11. **Rodamilans B**, **Valli A**, **Mingot A**, **San León D**, **Baulcombe D**, **López-Moya JJ**, **García JA**. 2015. RNA polymerase slippage as a mechanism for the production of frameshift gene products in plant viruses of the *Potyviridae* family. J Virol **89**:6965–6967.

12. **Olspert A**, **Chung BYW**, **Atkins JF**, **Carr JP**, **Firth AE**. 2015. Transcriptional slippage in the positive-sense RNA virus family *Potyviridae*. EMBO Rep **16**:995–1004.

13. **Hagiwara-Komoda Y**, **Choi SH**, **Sato M**, **Atsumi G**, **Abe J**, **Fukuda J**, **Honjo MN**, **Nakahara KS**, **Nagano AJ**, **Komoda K**, **Uyeda I**, **Naito S**. 2016. Truncated yet functional viral protein produced *via* RNA polymerase slippage implies underestimated coding capacity of RNA viruses. Sci Rep **6**:21411.

14. **Jayaram C**, **Hill JH**, **Miller WA**. 1992. Complete nucleotide sequences of two soybean mosaic virus strains differentiated by response of soybean containing the *Rsv* resistance gene. J Gen Virol **73**:2067–2077.

15. **Kaneko YH**, **Inukai T**, **Suehiro N**, **Natsuaki T**, **Masuta C**. 2004. Fine genetic mapping of the *TuNI* locus causing systemic veinal necrosis by turnip mosaic virus infection in *Arabidopsis thaliana*. Theor Appl Genet **110**:33–40.

16. **Hajimorad MR**, **Eggenberger AL**, **Hill JH**. 2003. Evolution of *Soybean mosaic virus*-G7 molecularly cloned genome in *Rsv1*-genotype soybean results in emergence of a mutant capable of evading *Rsv1*-mediated recognition. Virology **314**:497–509.

17. **Kim B**, **Masuta C**, **Matsuura H**, **Takahashi H**, **Inukai T**. 2008. Veinal necrosis induced by *Turnip mosaic virus* infection in *Arabidopsis* is a form of defense response accompanying HR-like cell death. Mol Plant Microbe Interact **21**:260–268.

18. **Liu J**, **Kim BM**, **Kaneko Y**, **Inukai T**, **Masuta C**. 2015. Identification of the *TuNI* gene causing systemic necrosis in *Arabidopsis* ecotype Ler infected with *Turnip mosaic virus* and characterization of its expression. J Gen Plant Pathol **81**:180–191.

19. **Wen RH**, **Khatabi B**, **Ashfield T**, **Saghai Maroof MA**, **Hajimorad MR**. 2013. The HC-Pro and P3 cistrons of an avirulent *Soybean mosaic virus* are recognized by different resistance genes at the complex *Rsv1* locus. Mol Plant Microbe Interact **26**:203–215.

20. **Atsumi G**, **Kagaya U**, **Kitazawa H**, **Nakahara KS**, **Uyeda I**. 2009. Activation of the salicylic acid signaling pathway enhances *Clover yellow vein virus* virulence in susceptible pea cultivars. Mol Plant Microbe Interact **22**:166–175.

21. **Ravelo G**, **Kagaya U**, **Inukai T**, **Sato M**, **Uyeda I**. 2007. Genetic analysis of lethal tip necrosis induced by *Clover yellow vein virus* infection in pea. J Gen Plant Pathol **73**:59–65.

22. **Yambao MLM**, **Yagihashi H**, **Sekiguchi H**, **Sekiguchi T**, **Sasaki T**, **Sato M**, **Atsumi G**, **Tacahashi Y**, **Nakahara KS**, **Uyeda I**. 2008. Point mutations in helper component protease of clover yellow vein virus are associated with the attenuation of RNA-

silencing suppression activity and symptom expression in broad bean. Arch Virol **153**:105–115.

23. **Masuta C**, **Yamana T**, **Tacahashi Y**, **Uyeda I**, **Sato M**, **Ueda S**, **Matsumura T**. 2000. Development of clover yellow vein virus as an efficient, stable gene-expression system for legume species. Plant J **23**:539–546.

24. **Hisa Y**, **Suzuki H**, **Atsumi G**, **Choi SH**, **Nakahara KS**, **Uyeda I**. 2014. P3N-PIPO of *Clover yellow vein virus* exacerbates symptoms in pea infected with *White clover mosaic virus* and is implicated in viral synergism. Virology **449**:200–206.

25. **Ido Y**, **Nakahara KS**, **Uyeda I**. 2012. *White clover mosaic virus*-induced gene silencing in pea. J Gen Plant Pathol **78**:127–132.

26. **Sato M**, **Masuta C**, **Uyeda I**. 2003. Natural resistance to *Clover yellow vein virus* in beans controlled by a single recessive locus. Mol Plant Microbe Interact **16**:994–1002.

27. **Nakahara KS**, **Nishino K**, **Uyeda I**. 2015. Construction of infectious cDNA clones derived from the potyviruses *Clover yellow vein virus* and *Bean yellow mosaic virus*. Methods Mol Biol **1236**:219–227.

28. **Edgar RC**. 2004. MUSCLE: multiple sequence alignment with high accuracy and high throughput. Nucleic Acids Res **32**:1792–1797.

29. **Chomczynski P**, **Sacchi N**. 1987. Single-step method of RNA isolation by acid guanidinium thiocyanate-phenol-chloroform extraction. Anal Biochem **162**:156–159.

30. **Atsumi G**, **Tomita R**, **Yamashita T**, **Sekine KT**. 2015. A novel virus transmitted through pollination causes ring-spot disease on gentian (*Gentiana triflora*) ovaries. J Gen Virol **96**:431–439.

31. **Aoyama T**, **Chua NH**. 1997. A glucocorticoid-mediated transcriptional induction system in transgenic plants. Plant J **11**:605–612.

896 32. **Atsumi G**, **Nakahara KS**, **Wada TS**, **Choi SH**, **Masuta C**, **Uyeda I**. 2012.
897 Heterologous expression of viral suppressors of RNA silencing complements virulence
898 of the HC-Pro mutant of clover yellow vein virus in pea. Arch Virol **157**:1019–1028.
899 33. **Laemmli UK**. 1970. Cleavage of structural proteins during the assembly of the head
900 of bacteriophage T4. Nature **227**:680–685.
901 34. **Sekine KT**, **Tomita R**, **Takeuchi S**, **Atsumi G**, **Saitoh H**, **Mizumoto H**, **Kiba A**,
902 **Yamaoka N**, **Nishiguchi M**, **Hikichi Y**, **Kobayashi K**. 2012. Functional
903 differentiation in the leucine-rich repeat domains of closely related plant virus-
904 resistance proteins that recognize common Avr proteins. Mol Plant Microbe Interact
905 **25**:1219–1229.
906 35. **Schneider CA**, **Rasband WS**, **Eliceiri KW**. 2012. NIH Image to ImageJ: 25 years of
907 image analysis. Nat Methods **9**:671–675.
908 36. **Tamura K**, **Stecher G**, **Peterson D**, **Filipski A**, **Kumar S**. 2013. MEGA6: Molecular
909 Evolutionary Genetics Analysis version 6.0. Mol Biol Evol **30**:2725–2729.
910 37. **Takahashi Y**, **Takahashi T**, **Uyeda I**. 1997. A cDNA clone to clover yellow vein
911 potyvirus genome is highly infectious. Virus Genes **14**:235–243.
912 38. **Wang Z**, **Ueda S**, **Uyeda I**, **Yagihashi H**, **Sekiguchi H**, **Tacahashi Y**, **Sato M**, **Ohya**
913 **K**, **Sugimoto C**, **Matsumura T**. 2003. Positional effect of gene insertion on genetic
914 stability of a clover yellow vein virus-based expression vector. J Gen Plant Pathol
915 **69**:327–334.
916 39. **Nakazono-Nagaoka E**, **Takahashi T**, **Shimizu T**, **Kosaka Y**, **Natsuaki T**, **Omura T**,
917 **Sasaya T**. 2009. Cross-protection against *Bean yellow mosaic virus* (BYMV) and
918 *Clover yellow vein virus* by attenuated BYMV isolate M11. Phytopathology **99**:251–
919 257.

40. **Wen RH**, **Maroof MAS**, **Hajimorad MR**. 2011. Amino acid changes in P3, and not the overlapping *pipo*-encoded protein, determine virulence of *Soybean mosaic virus* on functionally immune *Rsv1*-genotype soybean. Mol Plant Pathol **12**:799–807.

41. **Hjulsager CK**, **Olsen BS**, **Jensen DMK**, **Cordea MI**, **Krath BN**, **Johansen IE**, **Lund OS**. 2006. Multiple determinants in the coding region of *Pea seed-borne mosaic virus* P3 are involved in virulence against *sbm-2* resistance. Virology **355**:52–61.

42. **Andrade M**, **Sato M**, **Uyeda I**. 2007. Two resistance modes to *Clover yellow vein virus* in pea characterized by a green fluorescent protein-tagged virus. Phytopathology **97**:544–550.

43. **Kim BM**, **Suehiro N**, **Natsuaki T**, **Inukai T**, **Masuta C**. 2010. The P3 protein of *Turnip mosaic virus* can alone induce hypersensitive response-like cell death in *Arabidopsis thaliana* carrying *TuNI*. Mol Plant Microbe Interact **23**:144–152.

44. **Ozeki J**, **Takahashi S**, **Komatsu K**, **Kagiwada S**, **Yamashita K**, **Mori T**, **Hirata H**, **Yamaji Y**, **Ugaki M**, **Namba S**. 2006. A single amino acid in the RNA-dependent RNA polymerase of Plantago asiatica mosaic virus contributes to systemic necrosis. Arch Virol **151**:2067–2075.

45. **Komatsu K**, **Hashimoto M**, **Ozeki J**, **Yamaji Y**, **Maejima K**, **Senshu H**, **Himeno M**, **Okano Y**, **Kagiwada S**, **Namba S**. 2010. Viral-induced systemic necrosis in plants involves both programmed cell death and the inhibition of viral multiplication, which are regulated by independent pathways. Mol Plant Microbe Interact **23**:283–293.

46. **Komatsu K**, **Hashimoto M**, **Maejima K**, **Shiraishi T**, **Neriya Y**, **Miura C**, **Minato N**, **Okano Y**, **Sugawara K**, **Yamaji Y**, **Namba S**. 2011. A necrosis-inducing elicitor domain encoded by both symptomatic and asymptomatic *Plantago asiatica mosaic virus* isolates, whose expression is modulated by virus replication. Mol Plant Microbe Interact **24**:408–420.

945 47. **Anandalakshmi R**, **Pruss GJ**, **Ge X**, **Marathe R**, **Mallory AC**, **Smith TH**, **Vance**
946 **VB**. 1998. A viral suppressor of gene silencing in plants. Proc Natl Acad Sci USA
947 **95**:13079–13084.
948 48. **Cockerham G**. 1970. Genetical studies on resistance to potato virus X and Y.
949 Heredity **25**:309–348.
950 49. **Bendahmane A**, **Köhn BA**, **Dedi C**, **Baulcombe DC**. 1995. The coat protein of
951 potato virus X is a strain-specific elicitor of *Rx*1-mediated virus resistance in potato.
952 Plant J **8**:933–941.
953 50. **Bendahmane A**, **Kanyuka K**, **Baulcombe DC**. 1999. The *Rx* gene from potato
954 controls separate virus resistance and cell death responses. Plant Cell **11**:781–792.
955 51. **Baurès I**, **Candresse T**, **Leveau A**, **Bendahmane A**, **Sturbois B**. 2008. The *Rx* gene
956 confers resistance to a range of *Potexviruses* in transgenic *Nicotiana* plants. Mol Plant
957 Microbe Interact **21**:1154–1164.
958 52. **van der Hoorn RAL**, **Kamoun S**. 2008. From guard to decoy: a new model for
959 perception of plant pathogen effectors. Plant Cell **20**:2009–2017.
960 53. **Vijayapalani P**, **Maeshima M**, **Nagasaki-Takekuchi N**, **Miller WA**. 2012.
961 Interaction of the trans-frame potyvirus protein P3N-PIPO with host protein PCaP1
962 facilitates potyvirus movement. PLoS Pathog **8**:e1002639.
963 54. **Geng C**, **Cong QQ**, **Li XD**, **Mou AL**, **Gao R**, **Liu JL**, **Tian YP**. 2015.
964 Developmentally regulated plasma membrane protein of *Nicotiana benthamiana*
965 contributes to potyvirus movement and transports to plasmodesmata via the early
966 secretory pathway and the actomyosin system. Plant Physiol **167**:394–410.
967 55. **Cui X**, **Wei T**, **Chowda-Reddy RV**, **Sun G**, **Wang A**. 2010. The Tobacco etch virus
968 P3 protein forms mobile inclusions via the early secretory pathway and traffics along
969 actin microfilaments. Virology **397**:56–63.

970 56. **García-Arenal F**, **Fraile A**. 2013. Trade-offs in host range evolution of plant viruses.
971 Plant Pathology **62**:2–9
972 57. **Elena SF**, **Fraile A**, **García-Arenal F**. 2014. Evolution and emergence of plant
973 viruses. Adv Virus Res **88**:161–191.
974 58. **Lalić J**, **Cuevas JM**, **Elena SF**. 2011. Effect of host species on the distribution of
975 mutational fitness effects for an RNA virus. PLoS Genet **7**:e1002378–12.
976 59. **Fraile A**, **Pagán I**, **Anastasio G**, **Sáez E**, **García-Arenal F**. 2011. Rapid genetic
977 diversification and high fitness penalties associated with pathogenicity evolution in a
978 plant virus. Mol Biol Evol **28**:1425–1437.
979 60. **Fraile A**, **Hily JM**, **Pagán I**, **Pacios LF**, **García-Arenal F**. 2014. Host resistance
980 selects for traits unrelated to resistance-breaking that affect fitness in a plant virus. Mol
981 Biol Evol **31**:928–939.
982 61. **Jenner CE**, **Wang X**, **Ponz F**, **Walsh JA**. 2002. A fitness cost for *Turnip mosaic*
983 *virus* to overcome host resistance. Virus Research **86**:1–6.
984 62. **Khatabi B**, **Wen RH**, **Hajimorad MR**. 2013. Fitness penalty in susceptible host is
985 associated with virulence of *Soybean mosaic virus* on *Rsv1*-genotype soybean: a
986 consequence of perturbation of HC-Pro and not P3. Mol Plant Pathol **14**:885–897.
987 63. **Wang Y**, **Hajimorad MR**. 2015. Gain of virulence by *Soybean mosaic virus* on *Rsv4*-
988 genotype soybeans is associated with a relative fitness loss in a susceptible host. Mol
989 Plant Pathol. doi: 10.1111/mpp.12354.
990 64. **Quenouille J**, **Montarry J**, **Palloix A**, **Moury B**. 2013. Farther, slower, stronger: how
991 the plant genetic background protects a major resistance gene from breakdown. Mol
992 Plant Pathol **14**:109–118.

65. **Poulicard N**, **Pinel-Galzi A**, **Hébrard E**, **Fargette D**. 2010. Why *Rice yellow mottle virus*, a rapidly evolving RNA plant virus, is not efficient at breaking *rymv1-2* resistance. Mol Plant Pathol **11**:145–154.

66. **Miyashita, Y, Atsumi, G, Nakahara, KS.** 2016. Trade-offs for viruses in overcoming innate immunities in plants. Mol Plant Microbe Interact http://dx.doi.org/10.1094/MPMI-05-16-0103-CR

Figure legends

FIG 1 Mapping of the virulence determinant of Cl-90-1 Br2 in susceptible pea PI 226564. (A) Cl-90-1 Br2 or Cl-No.30 was inoculated and the symptoms were observed in inoculated leaf (a–c), upper uninoculated leaf (d–i), and whole plant (j,k). Photographs were taken at 14 (a–i), 17 (j), and 21 (k) days post inoculation (dpi). (B) Schematic representations of chimeric viruses constructed from Cl-90-1 Br2 (yellow) and Cl-No.30 (blue). Symptom severity in PI 226564 is indicated as the number of (+) symbols. We also show the infection profile in PI 429853 carrying recessive gene *cyv1,* which was reported in (7). Black triangles indicate positions of *GFP* insertion. (C) A series of chimeric viruses tagged with GFP were inoculated and the symptoms were monitored. Photographs were taken at 12 (a) and 17 (b) and 15 dpi (c; except for Cl-90-1 Br2 at 12 dpi) (D) Effect of *GFP* insertion into ClYVV on symptom development and virus accumulation. a, Cl-No.30 without *GFP*, with *GFP* between *P1* and *HC-Pro*, or with *GFP* between *NIb* and *CP* was inoculated onto PI 226564 (susceptible), and their symptoms were compared. b, Viral CP accumulation levels were compared by western blotting using antiserum against Cl-No.30 CP. The rbc-L band from the SDS-PAGE gel stained with Coomassie Brilliant Blue is shown as a loading control. (E) Comparison of symptoms among Cl-90-1 Br2, Cl-No.30, and Cl-RB without *GFP* at 21 dpi. (F) Virulence of

Cl-90-1 Br2-P3B$^{No.30}$, a Cl-90-1 Br2 mutant in which the P3B region in the 90-1 Br2 isolate was replaced with the corresponding region of Cl-No. 30. None of the viruses illustrated had a *GFP* insertion. The symptoms in a whole plant (a) and upper uninoculated leaf (b) are shown. Photographs were taken at 19 (a) and 13 (b) dpi. (G) Mapping of virulence determinants outside the P3B region. None of the chimeric viruses had a *GFP* insertion. The photograph was taken at 21 dpi.

FIG 2 Expression of P3 and/or P3N-PIPO from Cl-RB, Cl-No.30, and BY-CS in PI 226564 using a heterologous WClMV vector. (A) Schematic representations of *P3*, *P3N-PIPO*, and *P3ΔPIPO* constructs. The *P3* construct was expected to produce P3 accompanied by a small amount of P3N-PIPO as a frameshift product. *P3ΔPIPO* contained a mutation enabling it to produce P3 but not P3N-PIPO. *P3N-PIPO* had mutations for expressing P3N-PIPO in the zero frame but no P3. (B, C) *P3*, *P3N-PIPO*, and *P3ΔPIPO* constructs of Cl-RB (B) or Cl-No.30 (C) were expressed by WClMV vectors. The photographs in (B) and (C) were taken at 5 dpi. (D) *P3N-PIPO* of BY-CS was expressed by a WClMV vector. The photographs were taken at 14 dpi.

FIG 3 Multiple alignment of amino acid sequences of P3N-PIPO. Alignment was performed using the program MUSCLE (3.8) (http://www.ebi.ac.uk/Tools/msa/muscle/). Accession numbers: PSbMV-DPD1 (NC_001671), PSbMV-L1 (AJ252242), PSbMV-NEP1 (AJ311841), PSbMV-NY (X89997), ClYVV-I89-1 (LC096082), ClYVV-No.30 (AB011819), ClYVV-CYVV (HG970870), ClYVV-Gm (KF975894), ClYVV-90-1 Br2 (AB732962), BYMV-CS (AB373203), BYMV-90-2 (AB439731), BYMV-92-1 (AB439732), BYMV-GDD (AY192568), and BYMV-Vfaba2 (JN692500). The amino acid sequences of P3N-PIPO were obtained by translating the sequences from the 5′ end of *P3* to the stop codon of *P3N-PIPO*

1043 after introducing an A into the $A_{6\text{-}7}$ region in the $G_{1\text{-}2}A_{6\text{-}7}$ motif of each virus to shift the
1044 reading frame.
1045
1046 **FIG 4** Real-time PCR analysis of defense-associated gene expressions in susceptible PI
1047 226564. (A, B) SA-responsive (*SA-CHI*) and HR-associated (*HSR203J*) gene expressions in
1048 response to Cl-90-1 Br2, Cl-No.30, and BY-CS infections. Total RNA was extracted from the
1049 leaves (n=3) inoculated with Cl-90-1 Br2, Cl-No.30, and BY-CS at 6 dpi. cDNA was
1050 synthesized from total RNA and used for real-time PCR analysis. (C, D) *SA-CHI* expression
1051 in response to P3N-PIPO expression via WClMV. WClMV vectors carrying *P3N-PIPO*, *P3*,
1052 or *P3ΔPIPO* of Cl-RB (C), the corresponding genes from Cl-No.30 (D), *P3N-PIPO* from
1053 BY-CS (D), and *GFP* (C and D) as negative control were inoculated onto PI 226564. Total
1054 RNA was extracted from the inoculated leaves (n=3) at 4 dpi and used to synthesize cDNA
1055 for real-time PCR analysis. Expression levels of *SA-CHI* and *HSR203J* were normalized to
1056 that of *18S rRNA*. Fold changes from mock infection are shown. Error bars indicate standard
1057 deviations. Statistical analyses were conducted by the Tukey–Kramer method. Different
1058 letters above bars indicate statistically significant differences ($P < 0.05$ [A, B], $P < 0.01$ [C,
1059 D]).
1060
1061 **FIG 5** Comparison of the amount of P3N-PIPO produced from the *P3* cistron between Cl-RB
1062 and Cl-No.30 using an agroinfiltration assay in *N. benthamiana* leaf tissues. *P3(PIPO:FLAG*$^{-1}$*)*
1063 or *P3N-PIPO:FLAG*^{mk} of Cl-RB and Cl-No.30 were transiently expressed in the same leaf
1064 of *N. benthamiana*, and the production of protein from the PIPO frame was compared. (A)
1065 Schematic diagrams of plasmids for analyzing P3N-PIPO expression. To detect P3N-PIPO
1066 produced via frameshift to the −1 reading frame, we prepared the *P3(PIPO:FLAG*$^{-1}$*)*
1067 construct, in which a *FLAG* epitope tag sequence was inserted in front of the stop codon of

1068 the sequence encoding PIPO. *P3N-PIPO:FLAG*^{mk} has mutations that enable expression of
1069 P3N-PIPO tagged with FLAG in the zero frame. These modified *P3* cistrons were inserted in
1070 a binary vector between a DEX-inducible promoter and a poly(A) addition signal (pAs). (B)
1071 P3N-PIPO-FLAG accumulation was detected by western blotting using an antibody against
1072 FLAG. The numbers below the upper panel are relative band intensities of Cl-No.30
1073 compared with those of Cl-RB in each plant. Arrowheads indicate bands corresponding to
1074 P3N-PIPO. Yellow fluorescent protein was expressed as a negative control. (C) The level of
1075 *P3(PIPO:FLAG*$^{-1}$*)* mRNA was compared between Cl-RB and Cl-No.30 by real-time PCR
1076 analysis. The mRNA levels of *P3(PIPO:FLAG*$^{-1}$*)* were normalized to those of *EF1α*. The
1077 relative value for the *P3N-PIPO-FLAG* transcript of Cl-No.30 compared with that of Cl-RB
1078 is indicated for each plant. (D) Protein/mRNA ratios were calculated by dividing the relative
1079 value of protein (B) by that of mRNA (C) for each plant. (E–G) P3N-PIPO-FLAGs of Cl-RB
1080 and Cl-No.30 were expressed in the zero frame (*P3N-PIPO:FLAG*^{mk} of Cl-RB and Cl-No.30,
1081 respectively). The results in (E–G) are presented similarly to those shown in (B)–(D),
1082 respectively. Welch's *t*-test was applied to the data in D and G. * and ** indicates $P<0.05$ and
1083 $P<0.01$, respectively.
1084
1085 **FIG 6** Comparison of virus accumulation between Cl-No.30 and Cl-RB by using GFP-tagged
1086 viruses. (A) PI 226564 was inoculated with Cl-No.30/GFP and Cl-RB/GFP, and photographs
1087 of GFP fluorescence were taken at 5 dpi. Scale bar = 1 mm. (B) Comparison of virus
1088 accumulation per single infection focus at 5 dpi. Each sample was collected from 10 spots
1089 from five plants (2 spots/plant) and used for DAS-ELISA. Error bars indicate the standard
1090 deviations. Welch's *t*-test was applied to the data. *** indicates $P < 0.001$. (C) Comparison of
1091 virus cell-to-cell movement. GFP-fluorescent areas in inoculated leaves at 5 dpi were
1092 measured by ImageJ software. The areas of 50 spots from five plants (10 spots/plant) were

1093 measured for each virus. Error bars indicate the standard deviations. Welch's *t*-test was
1094 applied to the data. *** indicates $P < 0.001$.
1095
1096 **FIG 7** Mapping of the virulence determinant of Cl-90-1 in PI 226564. (A) Schematic
1097 representations of chimeric viruses constructed from Cl-No.30 (blue) and either Cl-90-1 Br2
1098 (yellow) or Cl-90-1 (yellow; sequence was not revealed in area with shaded yellow). Black
1099 triangles indicate the position of *GFP* insertion. Cl-RB^{M28R} has the P3B region of Cl-90-1,
1100 which contains an amino acid substitution (methionine to arginine) at position 28 of Cl-RB
1101 P3 (asterisk). The symptom severity in susceptible PI 226564 is indicated as the number of
1102 (+). We also show the infection profile in PI 429853 carrying recessive gene *cyv1*, which was
1103 reported in (7). (B) Alignment of amino acid sequences surrounding aa position 28 in P3. (C,
1104 D) Symptoms induced by Cl-RB^{M28R} were compared with those induced by Cl-RB. The
1105 photographs were taken at 14 (C) and 12 (D) dpi.
1106
1107 **FIG 8** *P3N-PIPO* expression by WClMV in PI 118501 and PI 429853. *P3N-PIPO-RB*, *P3N-*
1108 *PIPO-No.30*, and *P3N-PIPO-CS* were expressed by WClMV in PI 118501 (A) and PI
1109 429853 (B, C). The photographs were taken at 5 or 8 dpi, as indicated.
1110
1111 **FIG 9** Mapping of the region determining virulence in *P3N-PIPO* in PI 226564 and PI
1112 118501. *P3N^{CS}-PIPO^{RB}*, *P3N^{RB}-PIPO^{CS}* , *P3N-PIPO-RB*, *P3N-PIPO-CS*, and *GFP* were
1113 expressed by WClMV vectors in PI 226564 (A) and PI 118501 (B). *P3N^{CS}-PIPO^{RB}* has the
1114 *P3N* region of BY-CS and *PIPO* of Cl-RB; *P3N^{RB}-PIPO^{CS}* has the *P3N* region of Cl-RB and
1115 *PIPO* of BY-CS. Mock was treated with inoculation buffer only. The photographs of the
1116 inoculated leaves were taken at 8 dpi (A), 5 and 18 dpi (B). Lower panel in leftmost panels of

1117 A shows a magnified picture of the area indicated in upper panel. Arrowheads indicate
1118 regions in which cell death was induced.
1119
1120 **FIG 10** Gradation of virulence among ClYVVs and BYMV in susceptible and *cyv1*
1121 (recessive resistance) peas. (A) Symptoms were compared between Cl-90-1 Br2 and Cl-I89-1
1122 in PI 429853 (*cyv1*) at 25 dpi. The presence/absence of virus infection (by RT-PCR shown in
1123 B and C) is indicated below the photograph. (B) Cl-I89-1 and Cl-90-1 Br2 infections in upper
1124 uninoculated leaves (shown in A) were confirmed by RT-PCR at 25 dpi in PI 429853 (*cyv1*).
1125 (C) BY-CS infection in upper uninoculated leaves was confirmed by RT-PCR at 25 dpi in PI
1126 429853 (*cyv1*). For the positive control (p.c.), RT-PCR was done using an upper uninoculated
1127 leaf of PI 118501 inoculated with BY-CS. (D) The symptoms were compared between Cl-
1128 I89-1 and Cl-90-1 Br2 in PI 226564 at 10 dpi. (E) The symptoms were compared between Cl-
1129 No.30 (without *GFP*) and BY-CS in PI 226564 at 10 dpi. (F–H) Cl-I89-1, Cl-90-1 Br2, Cl-
1130 90-1, Cl-No.30, and BY-CS were inoculated onto PI 118501, and their symptoms were
1131 compared at 12 dpi. Upper symptomatic leaves of plants inoculated with BY-CS (G) or mock
1132 (H) are shown. (I) Gradation of virulence among ClYVVs and BYMV in recessive resistant
1133 (PI 429853 [*cyv1, Cyn1*]) (top graph) and susceptible (PI 226564 [weak *Cyn1*] and PI 118501
1134 [*Cyn1*]) (bottom graph) cultivars. The graphs indicate the consistent gradation observed in
1135 this study: the more efficiently a ClYVV isolate broke the resistance conferred by *cyv1* (top),
1136 the more it expressed virulence in susceptible peas (bottom). (J) Molecular phylogenetic
1137 analysis of full-length nucleotide sequences encoding polyprotein of ClYVV and BYMV.
1138 The sequences were aligned using MUSCLE and the maximum-likelihood tree was inferred
1139 using the MEGA6 package (36). The tree is drawn to scale, with branch lengths measured in
1140 the number of substitutions per site. TuMV-Tu-2R1 was set as an outgroup. The significance

1141 of the nodes was estimated with 1000 bootstrap replicates. The accession number of each
1142 virus is shown in Fig. 3 except for TuMV-Tu-2R1 (AB105135).
1143

TABLE 1 Summary of symptoms induced by ClYVV, BYMV, and WClMV expressing P3N-PIPO in pea[a]

Pea cultivar (genotype)	ClYVV				BYMV	WClMV[b]			
						ClYVV P3N-PIPO		BYMV P3N-PIPO	GFP
	I89-1	90-1 Br2	90-1	No.30	CS	90-1 Br2	No.30	CS	
PI 429853 (*Cyn1*[c], *cyv1*)	SCD[d]	No/CS[d]	No infection[d]	No infection[d]	No infection	Cell death	Cell death	Delayed cell death	No
PI 226564 (*Cyn*[e])	LSCD	LSCD	SCD	M/CS[fg]	M/CS[f]	Cell death	Cell death	No	No
PI 118501 (*Cyn1*)	LSCD	LSCD	LSCD	LSCD[fg]	M/CS[g]	Cell death	Cell death	Delayed cell death	No

[a] LSCD, lethal systemic cell death; SCD, systemic cell death; M, mosaic; CS, chlorotic spot; No, no symptoms.

[b] Cell death induction in the inoculated leaves was observed until 8 days after inoculation.

[c] Assumed to carry *Cyn1*

[d] (7).

[e] Putative weak *Cyn1* allele (20).

[f] (20).

[g] (21)

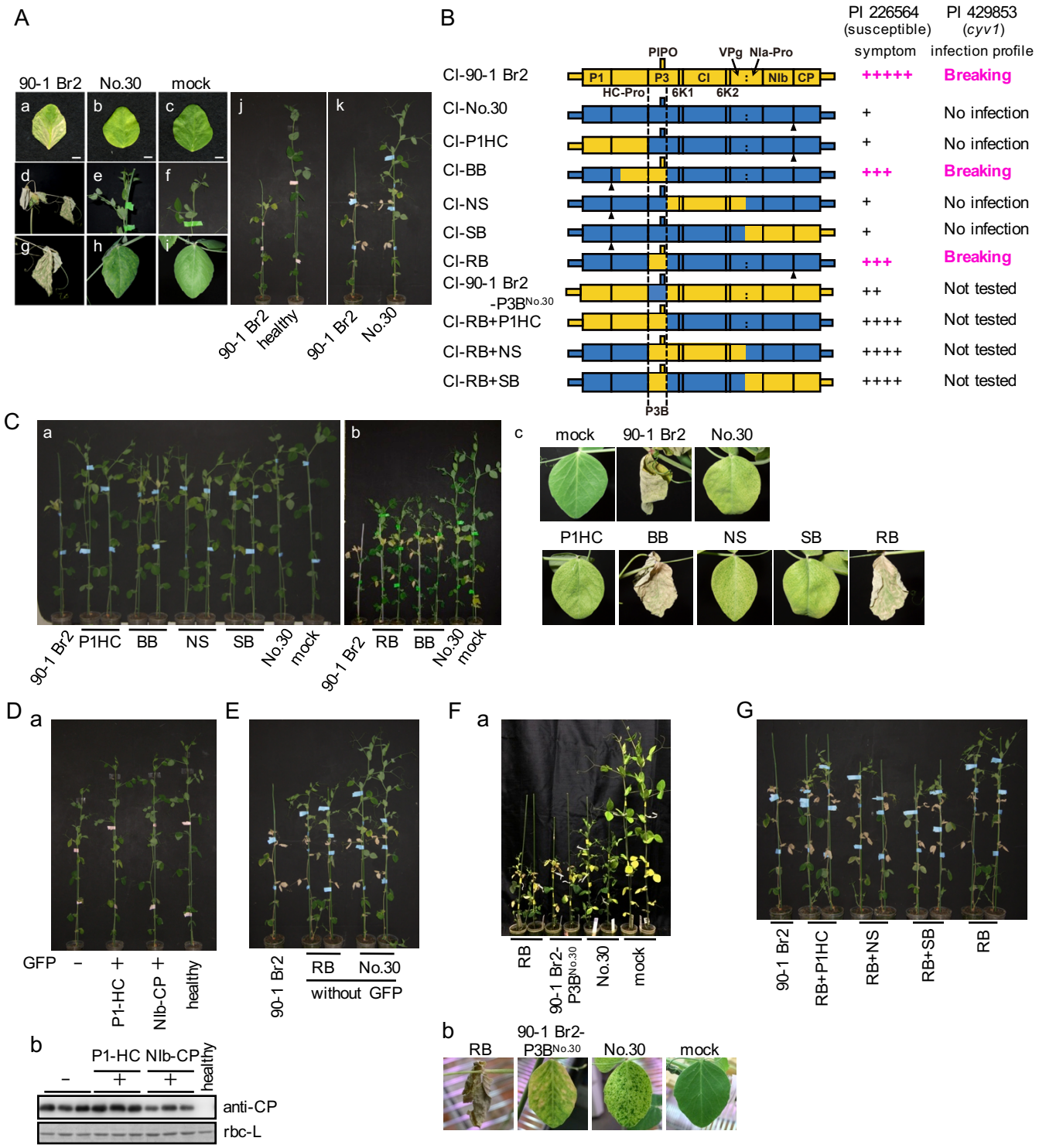
A
90-1 Br2
No.30
mock
a
b
c
d
e
f
g
h
i
j
k
90-1 Br2
healthy
90-1 Br2
No.30
B
PI 226564
(susceptible)
PI 429853
(cyv1)
symptom
infection profile
PIPO
VPg
Nla-Pro
P1
P3
CI
Nlb
CP
HC-Pro
6K1
6K2
CI-90-1 Br2
+++++
Breaking
CI-No.30
+
No infection
CI-P1HC
+
No infection
CI-BB
+++
Breaking
CI-NS
+
No infection
CI-SB
+
No infection
CI-RB
+++
Breaking
CI-90-1 Br2
-P3BNo.30
++
Not tested
CI-RB+P1HC
++++
Not tested
CI-RB+NS
++++
Not tested
CI-RB+SB
++++
Not tested
P3B
C
a
b
c
mock
90-1 Br2
No.30
P1HC
BB
NS
SB
RB
90-1 Br2
P1HC
BB
NS
SB
No.30
mock
90-1 Br2
RB
BB
No.30
mock
D
a
GFP
–
+
P1-HC
+
Nlb-CP
healthy
b
P1-HC
Nlb-CP
–
+
+
healthy
anti-CP
rbc-L
E
90-1 Br2
RB
No.30
without GFP
F
a
RB
90-1 Br2-
P3BNo.30
No.30
mock
b
RB
90-1 Br2-
P3BNo.30
No.30
mock
G
90-1 Br2
RB+P1HC
RB+NS
RB+SB
RB

FIG 1

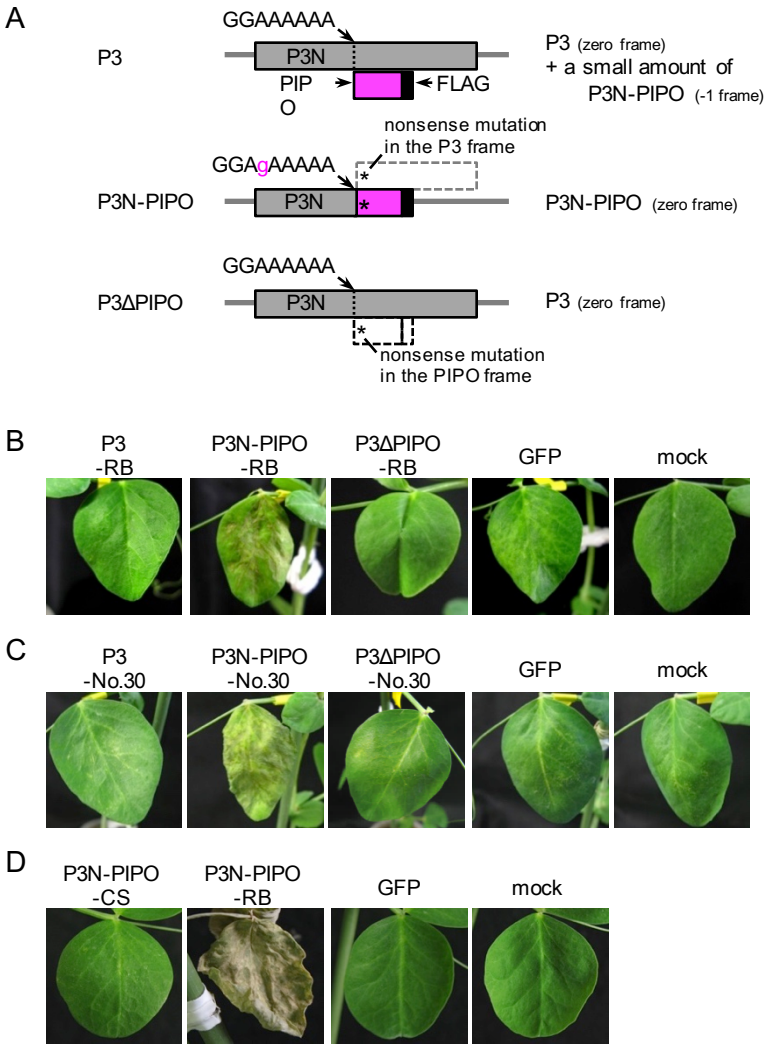
A
GGAAAAAA
P3
P3N
PIP
O
FLAG
P3 (zero frame)
+ a small amount of
P3N-PIPO (-1 frame)
nonsense mutation
in the P3 frame
GGAgAAAAA
P3N-PIPO
P3N
P3N-PIPO (zero frame)
GGAAAAAA
P3ΔPIPO
P3N
P3 (zero frame)
nonsense mutation
in the PIPO frame
B
P3
-RB
P3N-PIPO
-RB
P3ΔPIPO
-RB
GFP
mock
C
P3
-No.30
P3N-PIPO
-No.30
P3ΔPIPO
-No.30
GFP
mock
D
P3N-PIPO
-CS
P3N-PIPO
-RB
GFP
mock

FIG 2

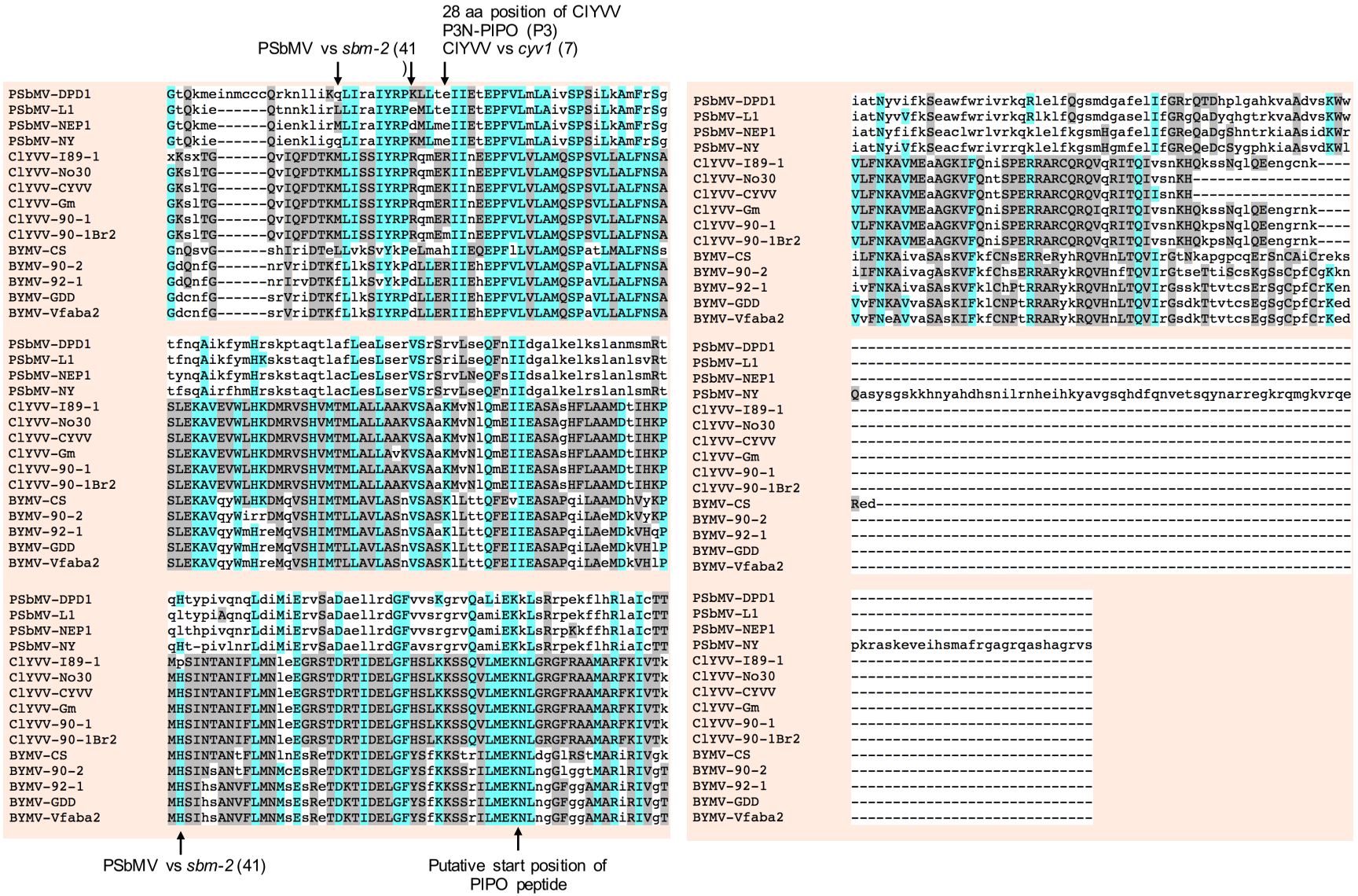
28 aa position of ClYVV
P3N-PIPO (P3)
PSbMV vs sbm-2 (41
ClYVV vs cyv1 (7)
PSbMV-DPD1
PSbMV-L1
PSbMV-NEP1
PSbMV-NY
ClYVV-I89-1
ClYVV-No30
ClYVV-CYVV
ClYVV-Gm
ClYVV-90-1
ClYVV-90-1Br2
BYMV-CS
BYMV-90-2
BYMV-92-1
BYMV-GDD
BYMV-Vfaba2
PSbMV vs sbm-2 (41)
Putative start position of
PIPO peptide

FIG 3

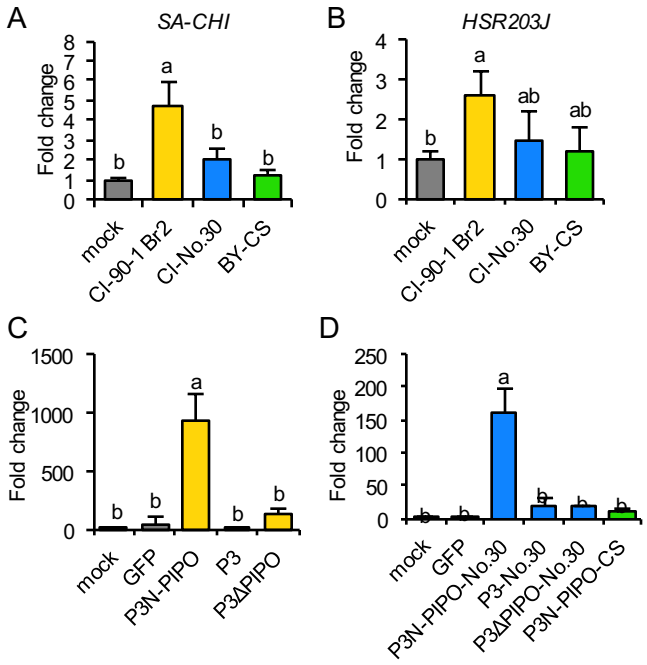
A
SA-CHI
Fold change
mock
Cl-90-1 Br2
Cl-No.30
BY-CS
B
HSR203J
Fold change
mock
Cl-90-1 Br2
Cl-No.30
BY-CS
C
Fold change
mock
GFP
P3N-PIPO
P3
P3ΔPIPO
D
Fold change
mock
GFP
P3N-PIPO-No.30
P3-No.30
P3ΔPIPO-No.30
P3N-PIPO-CS

FIG 4

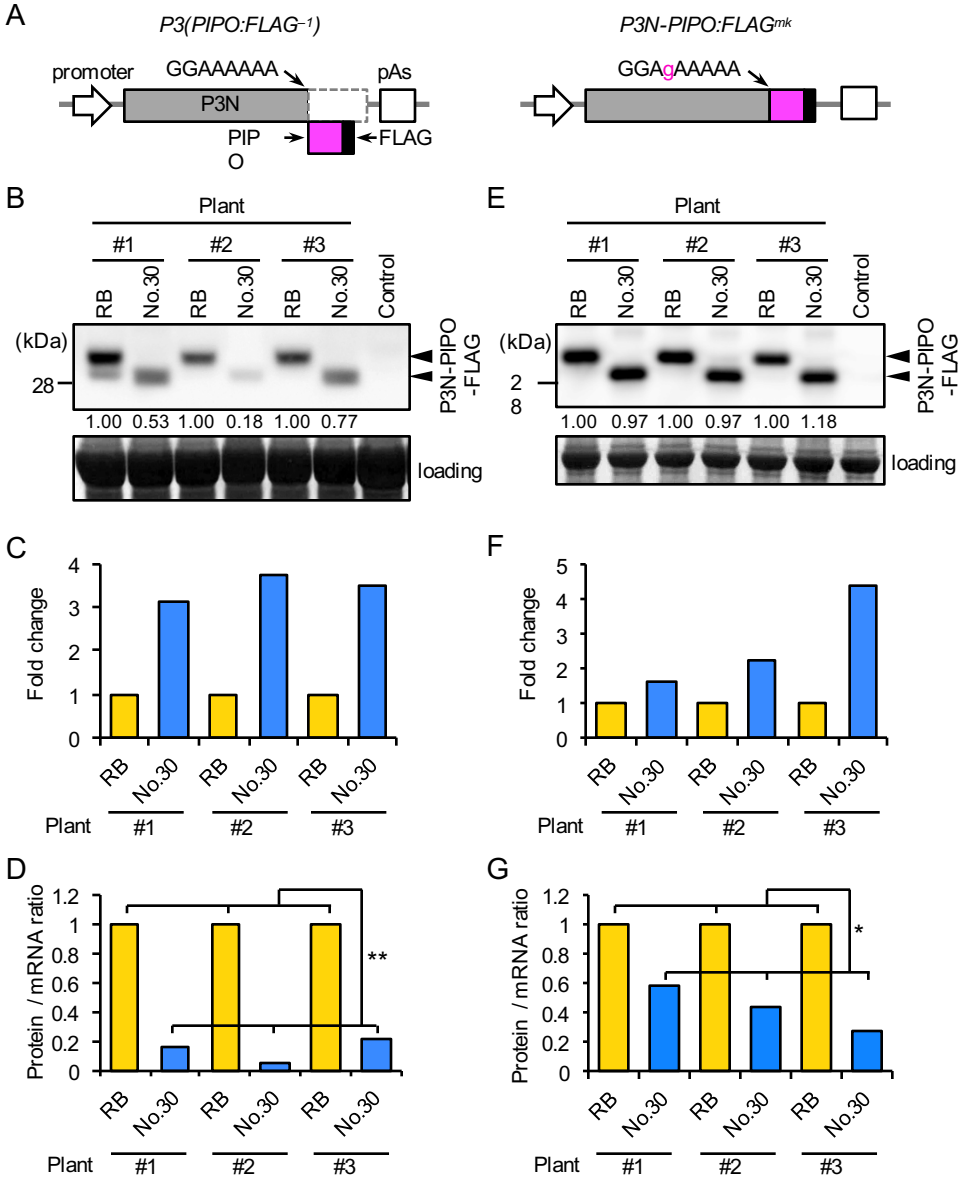
A
P3(PIPO:FLAG⁻¹)
promoter
GGAAAAAA
P3N
PIP
O
pAs
FLAG
P3N-PIPO:FLAGmk
GGAgAAAAA
B
Plant
#1
#2
#3
RB
No.30
Control
(kDa)
28
P3N-PIPO
-FLAG
1.00 0.53 1.00 0.18 1.00 0.77
loading
E
Plant
#1
#2
#3
RB
No.30
Control
(kDa)
2
8
P3N-PIPO
-FLAG
1.00 0.97 1.00 0.97 1.00 1.18
loading
C
Fold change
0
1
2
3
4
RB
No.30
Plant
#1
#2
#3
F
Fold change
0
1
2
3
4
5
RB
No.30
Plant
#1
#2
#3
D
Protein / mRNA ratio
0
0.2
0.4
0.6
0.8
1
1.2
**
RB
No.30
Plant
#1
#2
#3
G
Protein / mRNA ratio
0
0.2
0.4
0.6
0.8
1
1.2
*
RB
No.30
Plant
#1
#2
#3

FIG 5

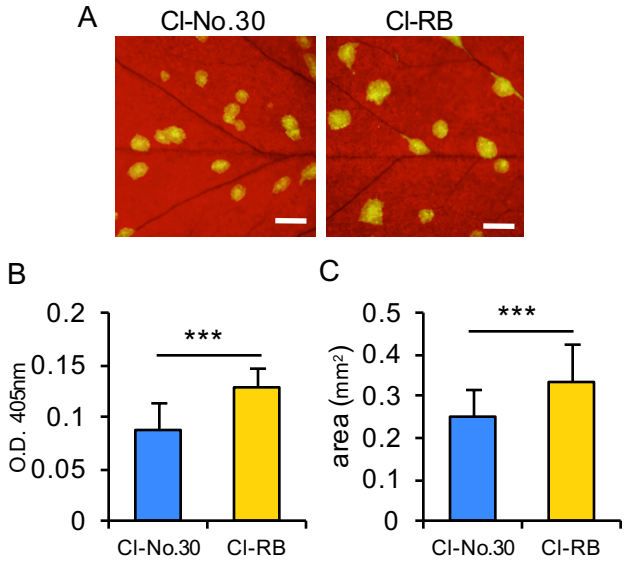
A
Cl-No.30
Cl-RB
B
O.D. 405nm
0.2
0.15
0.1
0.05
0
***
Cl-No.30
Cl-RB
C
area (mm²)
0.5
0.4
0.3
0.2
0.1
0
***
Cl-No.30
Cl-RB

FIG 6

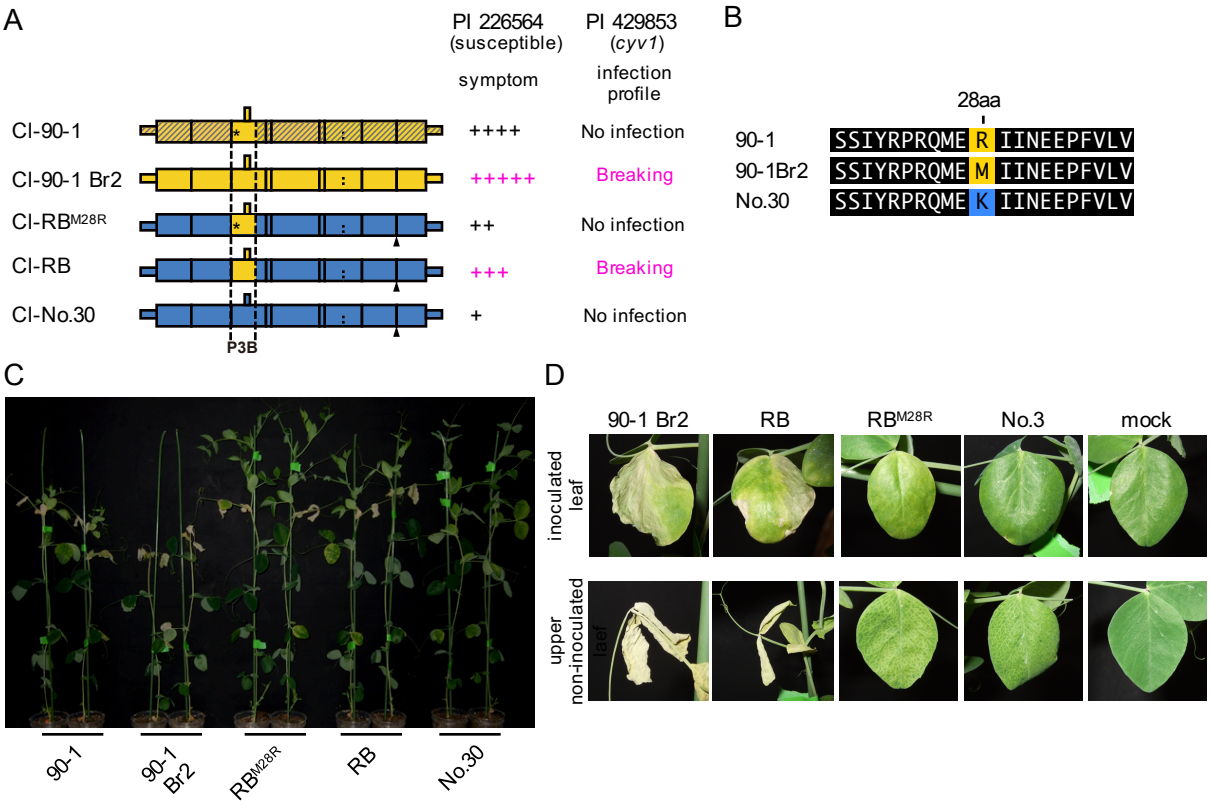
A
PI 226564
(susceptible)
PI 429853
(cyv1)
symptom
infection profile
Cl-90-1
++++
No infection
Cl-90-1 Br2
+++++
Breaking
Cl-RBM28R
++
No infection
Cl-RB
+++
Breaking
Cl-No.30
+
No infection
P3B
B
28aa
90-1
90-1Br2
No.30
SSIYRPRQME R IINEEPFVLV
SSIYRPRQME M IINEEPFVLV
SSIYRPRQME K IINEEPFVLV
C
90-1
90-1 Br2
RBM28R
RB
No.30
D
90-1 Br2
RB
RBM28R
No.3
mock
inoculated leaf
upper non-inoculated leaf

FIG 7

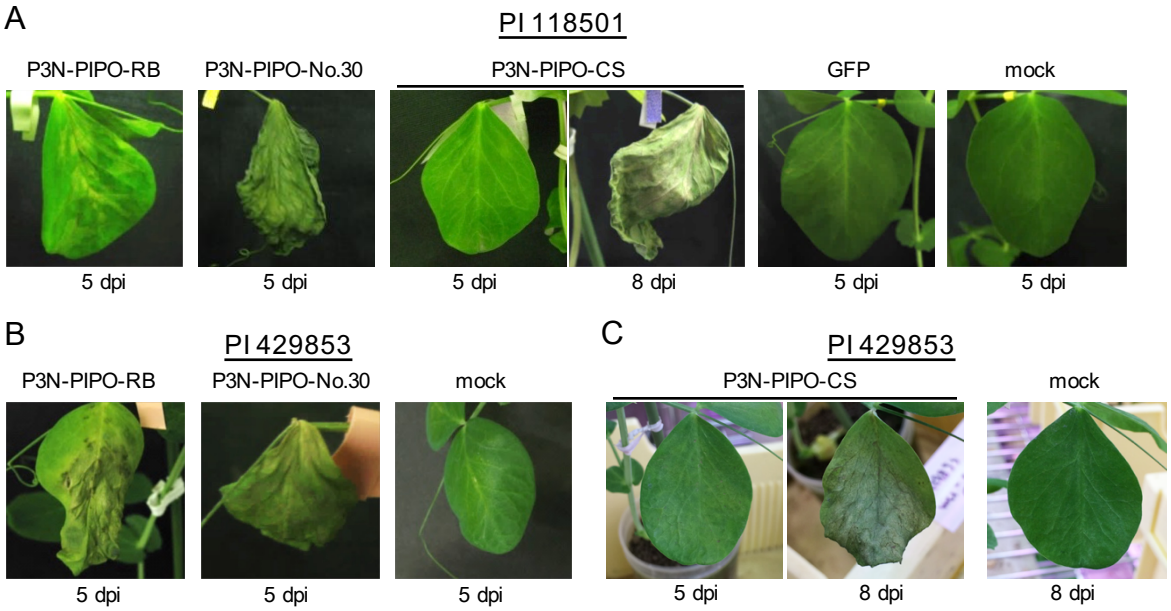
A
PI 118501
P3N-PIPO-RB
P3N-PIPO-No.30
P3N-PIPO-CS
GFP
mock
5 dpi
5 dpi
5 dpi
8 dpi
5 dpi
5 dpi
B
PI 429853
P3N-PIPO-RB
P3N-PIPO-No.30
mock
5 dpi
5 dpi
5 dpi
C
PI 429853
P3N-PIPO-CS
mock
5 dpi
8 dpi
8 dpi

FIG 8

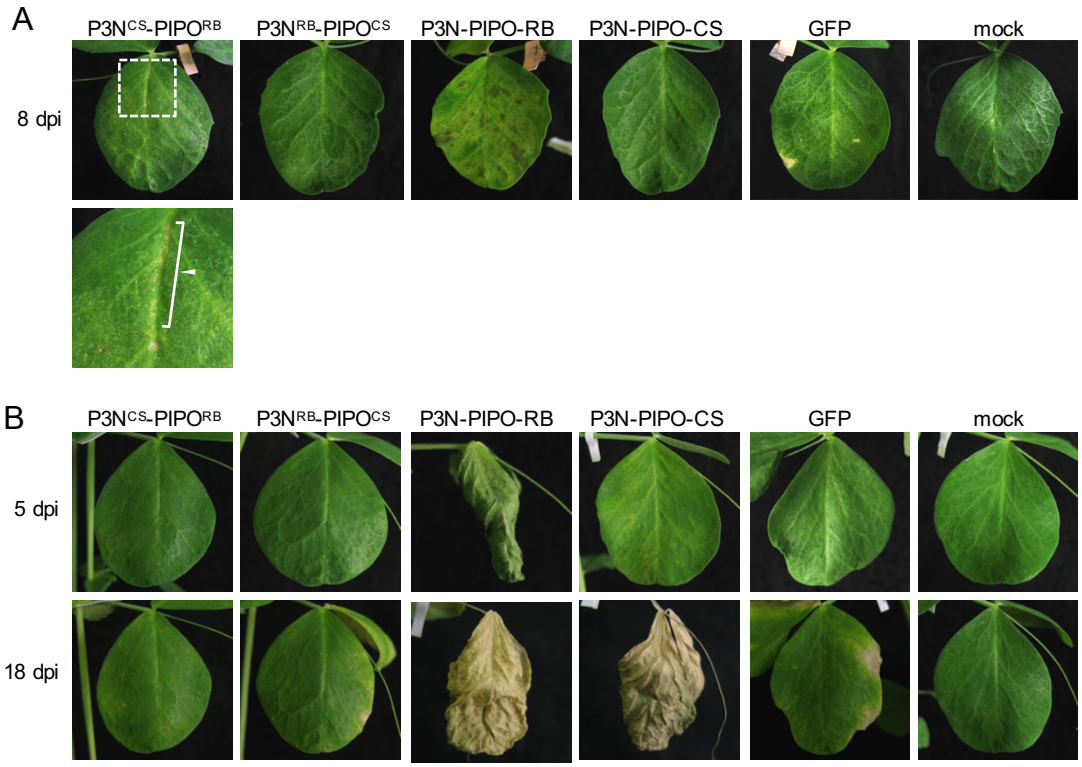
A
P3N^CS-PIPO^RB
P3N^RB-PIPO^CS
P3N-PIPO-RB
P3N-PIPO-CS
GFP
mock
8 dpi
B
P3N^CS-PIPO^RB
P3N^RB-PIPO^CS
P3N-PIPO-RB
P3N-PIPO-CS
GFP
mock
5 dpi
18 dpi

FIG 9

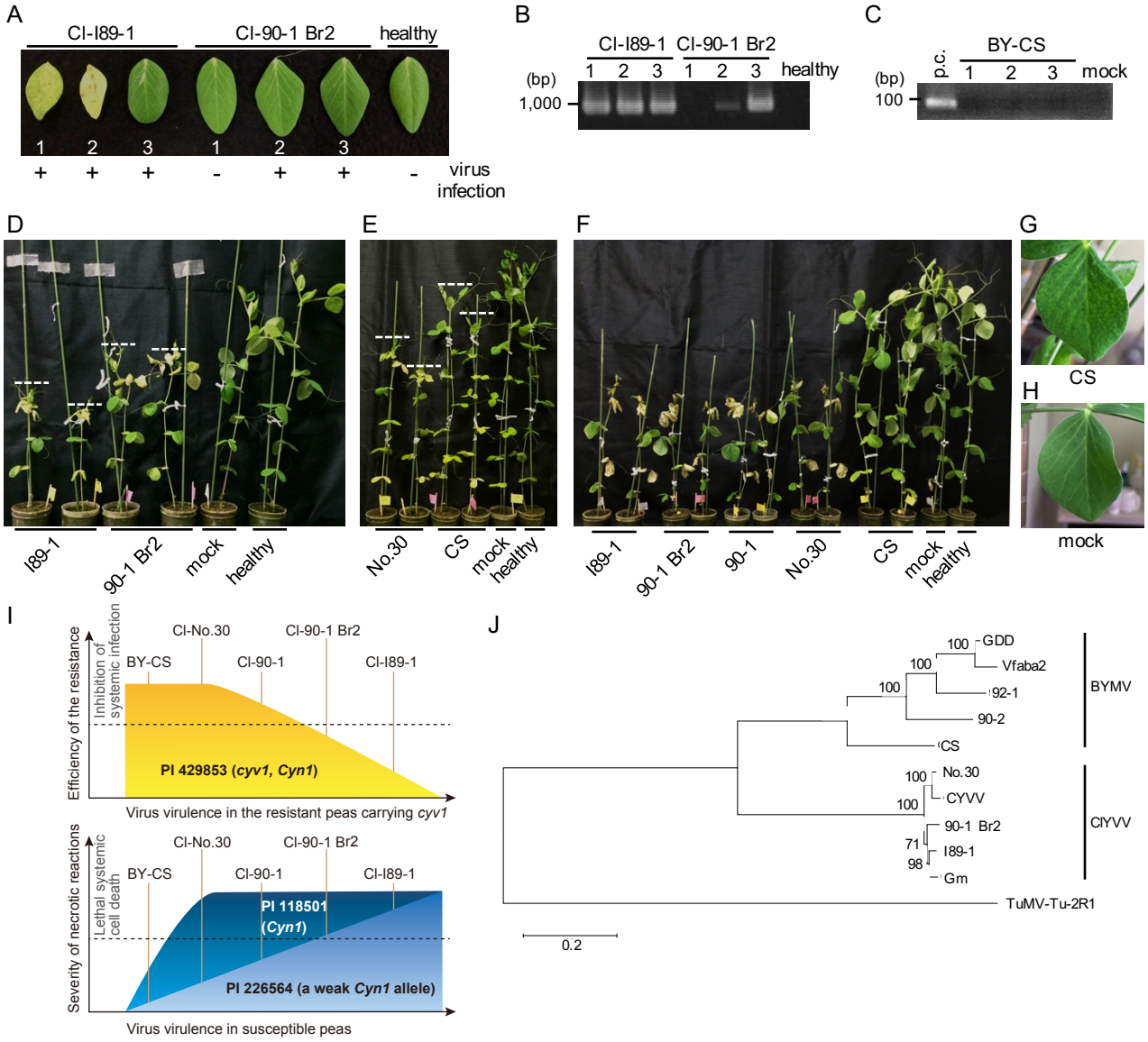
A
Cl-I89-1
Cl-90-1 Br2
healthy
1 2 3 1 2 3
+ + + - + + - virus infection
B
Cl-I89-1 Cl-90-1 Br2
1 2 3 1 2 3 healthy
(bp)
1,000
C
BY-CS
p.c.
1 2 3 mock
(bp)
100
D
I89-1
90-1 Br2
mock
healthy
E
No.30
CS
mock
healthy
F
I89-1
90-1 Br2
90-1
No.30
CS
mock
healthy
G
CS
H
mock
I
Efficiency of the resistance
Inhibition of systemic infection
BY-CS
Cl-No.30
Cl-90-1
Cl-90-1 Br2
Cl-I89-1
PI 429853 (cyv1, Cyn1)
Virus virulence in the resistant peas carrying cyv1
Severity of necrotic reactions
Lethal systemic cell death
PI 118501 (Cyn1)
PI 226564 (a weak Cyn1 allele)
Virus virulence in susceptible peas
J
100 GDD
100 Vfaba2
100 92-1
90-2
CS
100 No.30
100 CYVV
90-1 Br2
71 I89-1
98 Gm
TuMV-Tu-2R1
BYMV
ClYVV
0.2

FIG 10

FIG S1 Multiple alignment of nucleotide sequences of ClYVV and BYMV *P3* genes. Alignment was performed using the program MUSCLE (3.8) (http://www.ebi.ac.uk/Tools/msa/muscle/)(28). Accession numbers: BYMV-CS (AB373203), ClYVV-No.30 (AB011819), ClYVV-I89-1 (LC096082) and ClYVV-90-1 Br2 (AB732962). Red underline indicates the G_2A_6 motif. Red boxes indicate the stop codon of the PIPO reading frame in each sequence.